ITS UCDAVIS
INSTITUTE OF TRANSPORTATION STUDIES

Research Report – UCD-ITS-RR-08-56

Calibration of the *CalME* Rutting Model Using 2000 NCAT Data

March 2008

Rongzong Wu

Institute of Transportation Studies ◦ University of California, Davis
1605 Tilia Street ◦ Davis, California 95616
PHONE (530) 752-6548 ◦ FAX (530) 752-6572
www.its.ucdavis.edu

March 2008
Technical Memorandum: UCPRC-TM-2008-04

Calibration of the *CalME* Rutting Model Using 2000 NCAT Data

Author:
R. Wu

Partnered Pavement Research Program (PPRC) Contract Strategic Plan Element 4.1:
Development of Mechanistic-Empirical Design Method

PREPARED FOR:

California Department of Transportation
Division of Research and Innovation
Office of Roadway Research

PREPARED BY:

University of California
Pavement Research Center
UC Davis, UC Berkeley

DOCUMENT RETRIEVAL PAGE			Technical Memorandum: UCPRC-TM-2008-04
Title: Calibration of the *CalME* Rutting Model Using 2000 NCAT Data			
Author: R. Wu			
Caltrans Technical Lead: Imad Basheer			
Prepared for: Caltrans	**FHWA No.:** CA141080A	**Date Work Submitted:** March 13, 2008	**Date**: March 2008
Strategic Plan No.: 4.1	**Status:** Stage 6, final version		**Version No:** 1

Abstract:
CalME is a software package under development for Caltrans that is intended to help in the evaluation and design of flexible pavement structures. Building on existing design methods, *CalME* provides an Incremental-Recursive Mechanistic-Empirical (IRME) method in which the materials properties for the pavement are updated in terms of damage as the simulation of the pavement life progresses. The IRME design method incorporates various mathematical models to describe material behaviors and predict structure performances. These models need to be calibrated before they can be used to evaluate performance of different flexible pavement structures. This technical memorandum focuses on calibration of the incremental-recursive rutting model used in *CalME* when employing data collected during the APT (accelerated pavement testing) conducted in the first research cycle (years 2000–2002) at the NCAT (National Center for Asphalt Technology) pavement test track. It was found that the shift factor in *CalME* calibrated by rutting data in Heavy Vehicle Simulator tests led to a satisfactory match between calculated and measured rutting performance of the selected NCAT test sections.

Keywords:
CalME calibration, rutting, NCAT

Proposals for implementation:

Related documents:

Signatures:

R. Wu **First Author**	P. Ullidtz J. Signore **Technical Reviewers**	D. Spinner **Editor**	J. T. Harvey **Principal Investigator**	I. Basheer **Caltrans Technical Lead**	T. J. Holland **Caltrans Contract Manager**

DISCLAIMER STATEMENT

This document is disseminated in the interest of information exchange. The contents of this report reflect the views of the authors who are responsible for the facts and accuracy of the data presented herein. The contents do not necessarily reflect the official views or policies of the State of California or the Federal Highway Administration. This publication does not constitute a standard, specification or regulation. This report does not constitute an endorsement by the Department of any product described herein.

For individuals with sensory disabilities, this document is available in Braille, large print, audiocassette, or compact disk. To obtain a copy of this document in one of these alternate formats, please contact: the Division of Research and Innovation, MS-83, California Department of Transportation, P.O. Box 942873, Sacramento, CA 94273-0001.

PROJECT OBJECTIVES

The study presented in this tech memo is part of Partnered Pavement Research Center Strategic Plan Element 4.1, whose objective is to evaluate and develop mechanistic-empirical design procedures for California. The study presented in this tech memo provides a calibration and validation of the asphalt mix rutting model used in *CalME,* which is the new mechanistic-empirical flexible pavement design software under development by UCPRC for Caltrans.

TABLE OF CONTENTS

LIST OF FIGURES

LIST OF TABLES

1 INTRODUCTION

1.1. Background and Objective

CalME is a software package developed for Caltrans to help in the evaluation and design of flexible pavement structures (*1*). Building on existing design methods, *CalME* provides an Incremental-Recursive Mechanistic-Empirical (IRME) method in which the materials properties for the pavement are updated in terms of damage as the pavement life simulation progresses. The IRME design method incorporates various mathematical models to describe materials' behaviors and predict structure performances. These models must be calibrated before they can be used to evaluate the performance of different flexible pavement structures.

The objective of the work presented in this technical memorandum focuses on calibration of the incremental-recursive rutting model used in *CalME* and employing data collected during the APT (accelerated pavement testing) conducted in the first research cycle at the NCAT (National Center for Asphalt Technology) pavement test track. This research cycle is referred to in this memo as the 2000 NCAT Test, to indicate its starting year.

CalME is under continuous development. Version 0.6-20071111 of *CalME* was used in this calibration study.

This work was performed as part of Partnered Pavement Research Center Strategic Plan Element 4.1, titled "Development of the First Version of a Mechanistic-Empirical Pavement Rehabilitation, Reconstruction, and New Pavement Design Procedure for Rigid and Flexible Pavements." This work is being performed under the technical oversight of the Caltrans Mechanistic-Empirical Design Task Group, led by the Division of Design.

1.2. Tech Memo Organization

This tech memo presents a summary of the model calibration study and is organized as follows:

- Chapter 2 provides brief descriptions of the NCAT test facility and the selection of test sections.
- Chapter 3 presents models used by *CalME* in the study.
- Chapter 4 presents and discusses the collection of the necessary data for running *CalME.*
- Chapter 5 presents details on how *CalME* was run to simulate track tests.
- Chapter 6 provides results and discusses them.
- Chapter 7 presents conclusions reached from the calibration study.

2 NCAT PAVEMENT TEST TRACK

2.1 Overview

The NCAT pavement test track (the Test Track) is a 2.8 km (1.7 mi) long oval-shaped closed-loop facility managed by NCAT. The test track is divided into 46 experimental sections, each 60 m (200 ft) long (*2*). An aerial view of the test track is shown in Figure 2.1. A layout of the experiment sections is shown in Figure 2.2.

Figure 2.1: Overview of the NCAT track facility.
(Taken from the photo album on the NCAT website: *www.pavetrack.com/images/photo%20album/).*

The NCAT track is the result of a joint effort of industry and government to improve the quality of flexible pavements. The Alabama Department of Transportation (ALDOT) funded the construction of the track at NCAT. Experimental sections of the test track are cooperatively funded by external sponsors, most commonly state DOTs, with subsequent operation and research managed by NCAT (*3*).

Tests at the NCAT test track were conducted in three-year cycles starting in 2000. The data used in this study are from the first research cycle, which began in 2000 and ended in 2003, during which a total of 10,000,000 equivalent single-axle loads (ESALs) were applied over a two-year period, with pavement performance documented regularly. The first research cycle at the NCAT test track is referred to herein as the 2000 NCAT Test.

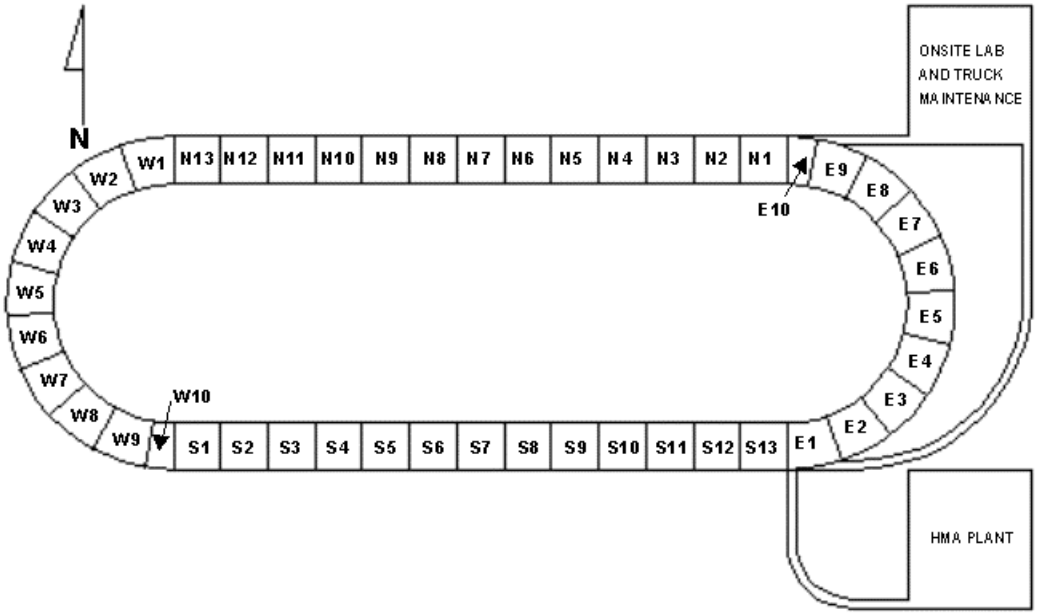

Figure 2.2: NCAT pavement test track experiment section layout.
(Sections are named using a letter to indicate quadrate and a number to indicate sequence).

For the 2000 NCAT test, the underlying structural buildup was exactly the same for every section, with sponsors typically choosing to place their research mixes at a total thickness of 100 mm (4 inches) to facilitate direct comparisons with other sponsors' results. The underlying pavement structure was relatively thick to avoid fatigue failures. The final buildup, which was developed by ALDOT under the supervision of the oversight committee, consisted of (from the bottom up) on-site common subgrade (the same under all test sections), 150 mm of dense crushed aggregate base, 125 mm of permeable asphalt-treated base, 225 mm of Superpave lower base mix (produced with unmodified asphalt), 150 mm of Superpave upper base mix (produced with modified asphalt), and finally 100 mm of experimental mix (typically placed as a 50 mm binder mix under a 50 mm surface mix) (*2*). The entire track is underlain by edge drains that run along both the inside and outside edges of the pavement structure, fed by water from the permeable asphalt-treated base as well as by water that leaches in from the shoulders.

Mix characteristics for the sections used in this study can be found in the construction report (*4*) and the mix designs are summarized in Appendix A. The on-site common silty-clay subgrade, classified as an AASHTO A-4(0) soil, had an average stiffness of 220 MPa (32 ksi) based on backcalculation using falling weight deflectometer data.

Table 2.1: Structure of First Research Cycle NCAT Test Pavements

Layer Number	Layer Type	Description	Thickness (mm)
1	AC	Experimental mix	100
2	AC upper base	Superpave mix with modified binder	150
3	AC bottom base	Superpave mix with unmodified binder	225
4	ATPB base	Asphalt-treated permeable base	125
5	AB	Dense crushed aggregate base	150
6	SG	On-site common subgrade	–

2.1 Calibration Section Selection

The materials stiffnesses and performance equation coefficients used in *CalME* require laboratory testing. The rutting equation parameters are based on the repeated simple shear test at constant height (RSST-CH). It was decided to choose only four sections in this study, owing to the time commitment needed on the part of the UCPRC laboratory to test more than that number of sections. The criteria for choosing a test section for calibration included the following factors:

- Performance data must have already been released.
- Sufficient material must be available to perform the RSST-CH tests.
- A relatively large amount of rutting is required.

None of the sections in the 2000 NCAT Test experienced a large amount of rutting; the maximum total rutting measured at the conclusion of the tests was about 8 mm. It was decided to use data from Sections N4, N6, N8, and N9 for calibrating *CalME*. These four sections include modified and unmodified binders in the surface asphalt concrete (AC) layer.

3 *CalME* MODELS USED

This chapter describes the theoretical model used for various components of the pavement in *CalME* for this study. Note that the models may be changed in future versions of the software. These models are described in the help file CalME_Help_File.chm or CalME.pdf under the installation folder for *CalME,* which typically is "C:\Program Files\CalME."

In particular, no fatigue models are involved. In other words, fatigue model parameters were set in such a way that none of the layers would experience fatigue damage. This is because the pavement was built with a very strong underlying support composed of two lifts of AC base (375 mm in total thickness) and a 125 mm ATPB layer, followed by regular aggregate base and subgrade. No fatigue cracking was observed (*3*) for any of the test sections, and accordingly the fatigue damage was assumed to be too small to affect the rutting result.

3.1 Asphalt-Bound Layer Models

Asphalt-bound materials in the NCAT Test Track include the top four layers (see Table 2.1). The models used in this study include modulus model and rutting model.

3.1.1 Material Modulus

Asphalt-bound material modulus was determined as a function of temperature and loading time, using the National Cooperative Highway Research Program (NCHRP) 1-37A Design Guide model (*5*):

$$\log(E) = \delta + \frac{\alpha}{1 + \exp(\beta + \gamma \log(tr))} \quad \textbf{(1)}$$

where E is the modulus in MPa,
tr is reduced time in sec,
α, β, γ, and δ are constants, and
logarithms are to base 10.

Reduced time is found from:

$$tr = lt \times \left(\frac{visc_{ref}}{visc} \right)^{aTg} \quad \textbf{(2)}$$

where *lt* is the loading time (in sec),
$visc_{ref}$ is the binder viscosity at the reference temperature,
visc is the binder viscosity at the present temperature, and
aTg is a constant.

Binder viscosity can be calculated from temperature by using the following equation:

$$\log(\log visc\ cPoise) = A + VTS \cdot \log T_k \quad \textbf{(3)}$$

where T_k is binder temperature in Kelvin, A = 9.6307, and VTS = -3.5047.

3.1.2 Rutting Model

A shear-based approach, developed by Deacon et al. (*6*) for predicting rutting of the asphalt layer, was used in a first attempt. Rutting in the asphalt is assumed to be controlled by shear deformation. The rutting estimates used computed values of shear stress, τ, and elastic shear strain, γ^e, at a depth of 50 mm beneath the edge of the tire. It was also assumed in this approach that rutting occurs solely in the top 100 mm of AC layer.

Rutting in the AC layer due to the shear deformation is determined from the following:

$$rd_{AC}\ mm = K \times \gamma^i \times h \quad \textbf{(4)}$$

where $rd_{AC}\ mm$ is the vertical rut depth in the asphalt concrete,
γ^i is permanent (inelastic) shear strain at 50 mm depth,
K is a value relating permanent shear strain to rut depth (mm), and
h is the thickness of AC layer in millimeters with a maximum value of 100 mm.

The permanent strain may be calculated from a gamma function (type "g" in *CalME*):

$$\gamma^i = \exp\left(A + \alpha \times \left[1 - \exp\left(-\ln(N)/\gamma \right) \times \left(1 + \ln(N)/\gamma \right) \right] \right) \times \exp\left(\beta \times \tau / \tau_{ref} \right) \times \gamma^e \quad \textbf{(5)}$$

where τ =shear stress determined at this depth using elastic analysis,
γ^e = corresponding elastic shear strain (m/m),
N = equivalent number of load repetitions, which is the number of load repetitions at the stress and strain level of the next time increment to reach the permanent shear strain calculated at end of current time increment, and
A, α, β, γ, and τ_{ref} are constants.

Or a power function (type "t" in *CalME*):

$$\gamma^i = A \times MN^{\alpha} \exp\left(\frac{\beta \times \tau}{\tau_{ref}} \right) \times \left(\gamma^e \right)^{\gamma} \quad \textbf{(6)}$$

where MN is the equivalent number of load repetitions defined in Equation (5) but is expressed in millions.

3.2 Unbound Material Models

Two types of unbound materials were used in the NCAT test track: the dense crushed aggregate base and the common on-site subgrade. The subgrade was compacted from materials excavated from a borrow-pit located at the west curve of the test track.

3.2.1 Material Modulus

Unbound materials are treated as linear elastic material with constant stiffness and Poisson ratio.

3.2.2 Permanent Deformation

Permanent deformation, d_p, of the unbound materials is based on the vertical resilient strain at the top of the layer, ε, and on the modulus of the material, E:

$$d_p = A \times MN^{\alpha} \times \left(\frac{\varepsilon}{\varepsilon_{ref}} \right)^{\beta} \times \left(\frac{E}{E_{ref}} \right)^{\gamma} \quad \textbf{(7)}$$

where d_p= permanent deformation (mm) of an unbound layer,
MN = number of load repetitions in millions,
A, α, β, γ, ε_{ref}, and E_{ref} are constants.

The model was developed based results from a test road where the Danish Road Testing Machine was used between 1994 and 1997) (Appendix B). This model is designated as type "e" for permament deformation in *CalME*.

4 DATA COLLECTION

4.1 Introduction

Data needed for *CalME* model calibration can be grouped into four major categories: environment, traffic, structure, and performance. The first three data groups provide necessary inputs for running *CalME,* while the last group provides measured results that help when calibrating empirical shift factors used in *CalME* so that the calculated performance can match the measured values.

Most of the data were collected from the NCAT web site *(http://spider.eng.auburn.edu/ncat/db/ncat.html),* which allows for exporting data from the test track database maintained by NCAT. Descriptions of the 2000 NCAT Test can be found in (*2*). This chapter describes how the model parameters were determined, using various sources of data collected.

4.2 Environment

Environmental conditions refer to temperatures of the pavement and moisture contents of both aggregate base and subgrade. These conditions affect layer stiffness. Temperatures and moisture contents were measured by NCAT.

4.2.1 Temperatures

Each individual section on the 2000 NCAT Track was outfitted with multi-depth temperature instrumentation, as shown schematically in Figure 4.1. Temperature data were automatically collected using Compbell CR10X data-logging computers (mounted along the perimeter of the track) that record hourly average, minimum, and maximum values. Temperatures were measured via precision thermisters installed during construction at depths of 0, 50, 100, and 250 mm. In general, temperature sensors performed well through the end of the project even though minor issues were identified for certain sections.

Each of the 23 CR10X enclosures was mounted on the back of every other section sign around the track's perimeter in such a way that the section shared a data logger with the adjacent section. Temperature data for every two adjacent sections are saved in one table in the NCAT database, with one set of data labeled as "Left section" and another as "Right section." Because the section signs were installed along the outer perimeter of the test track, the "Left section" was assumed to be the section that had a smaller sequence number, while the "Right section" referred to the one with a larger sequence number. The temperature data sources for the four sections selected are listed in Table 4.1.

Table 4.1: Section Temperature Data Source

Section	NCAT Table Name	Section Identification
N4	LAYTEMP_N3N4_2000	Right section
N6	LAYTEMP_N5N6_2000	Right section
N8	LAYTEMP_N7N8_2000	Right section
N9	LAYTEMP_N9N10_2000	Left section

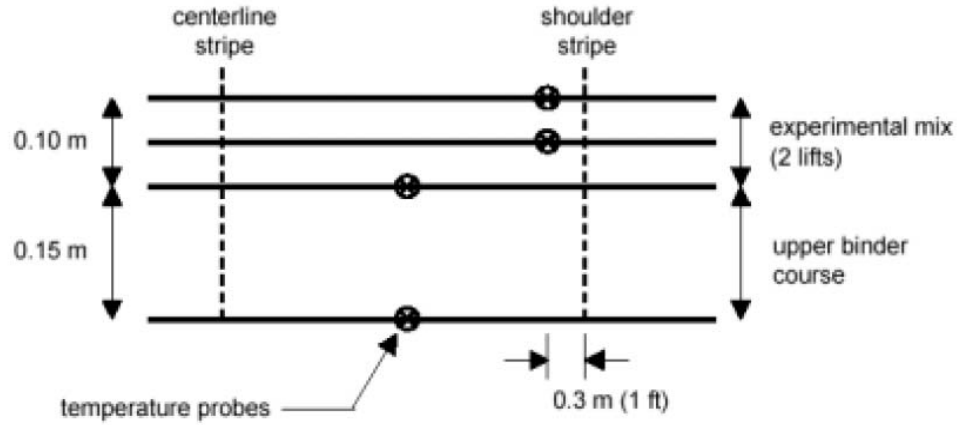

Figure 4.1: Multidepth temperature measurement configuration.

After inspection of the temperature data, the following issues were found:

1. Temperatures for "Left section" are very different from the ones for "Right section" that were recorded in the same data table. The right sections showed consistently larger daily variation than the left sections.
2. The depth specifications in the database seem to be erroneous because the data indicated unreasonable timing in daily temperature change (specifically, temperature at deeper locations rose earlier than the surface temperature). Also, on some occasions the temperatures at deeper locations showed larger daily variation than surface temperature.
3. There were gaps in the temperature record when truck trafficking was applied.

It is believed that adjacent sections should have similar temperatures, since the pavement structures were the same and materials used were very similar. To determine whether "Left section" temperatures or "Right section" temperatures should be used, both were compared to the pavement temperatures recorded for the 2003 NCAT test (i.e., the second APT research cycle at NCAT). An example of such comparison is shown in Figure 4.2, in which the 2003 NCAT test temperature data for Sections N3 and N4 were plotted along with the 2000 test data, with the year stamp for 2003 data shifted to align with the 2000 data.

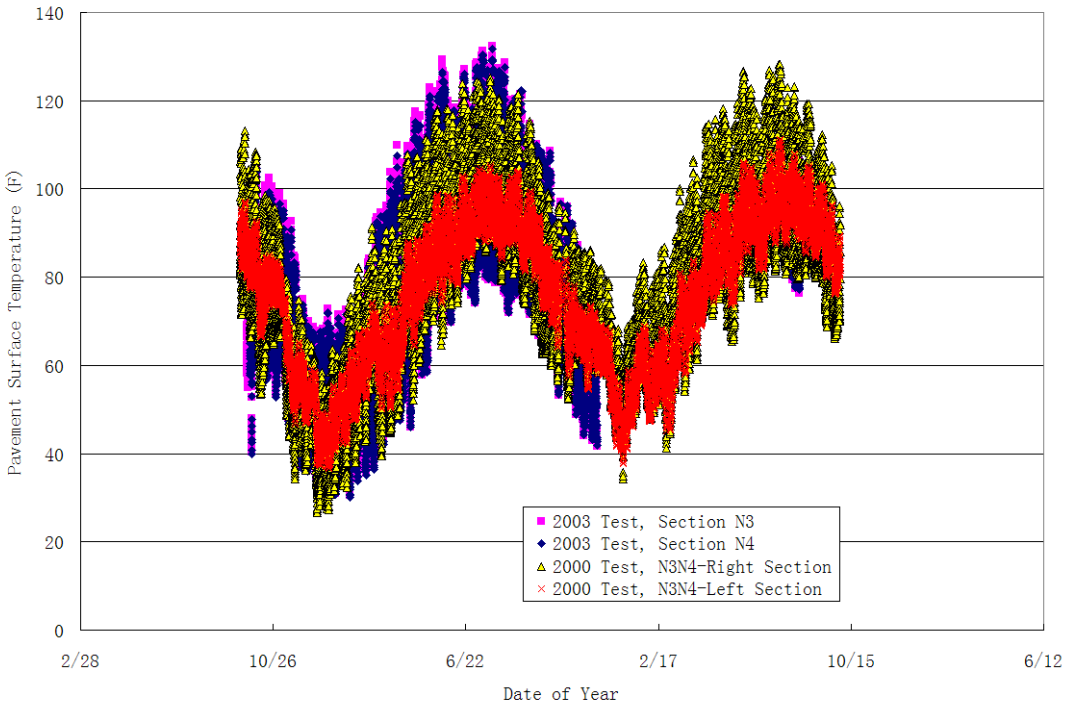

Figure 4.2: Comparison of pavement surface temperature records.

As shown in Figure 4.2, pavement surface temperatures for Sections N3 and N4 in the 2003 NCAT test were quite similar, which confirmed that temperatures for adjacent sections were roughly the same. Furthermore, temperatures for the "N3N4-Right section" in the 2000 NCAT test were quite similar to the 2003 temperatures but were very different from the "N3N4-Left section" in the 2000 NCAT test. These observations apply to other sections as well, which suggests that temperatures recorded for the "Right sections" were correct and therefore were used in this study.

To identify the correct depths for multiple thermisters installed within a given section, the instruments were sorted based on the daily variation of temperatures that each recorded. It was assumed that daily temperature variation decreases with an increase in depth. It was verified that thermisters showing smaller recorded daily temperature variations also heated up later than the ones with larger recorded variations. The actual thermister depths, corresponding to the numbering used in the database, are listed in Table 4.2.

The gaps in temperature record were filled using temperatures recorded for either the previous year or previous day, depending on data availability.

Table 4.2: Actual Depths for Thermisters in Various Sections

Section	No. 1	No. 2	No. 3	No. 4
N4	100	50	250	0
N6	0	50	100	250
N8	250	50	100	0
N9	100	0	250	50

It was found that temperatures for the four sections selected were very similar. It was therefore decided to use the average temperatures over the four sections in the actual *CalME* simulations. The final temperatures used are shown in Figure 4.3. In addition to the temperatures shown in the figure, an additional imaginary thermister with a depth of 2,000 mm and a constant temperature of 24.1°C was set in *CalME*. That allowed the software to obtain temperatures for all the necessary calculation points below 250 mm.

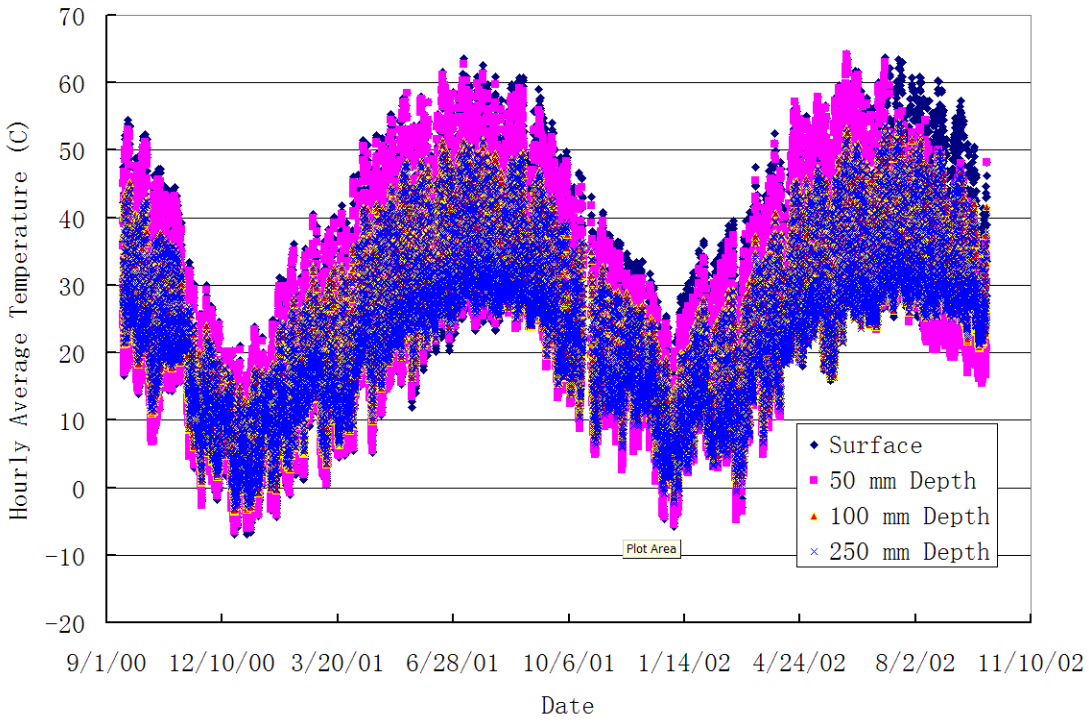

Figure 4.3: Pavement temperatures used in *CalME* simulation.
(An additional temperature of 24.1°C was set for 2,000 mm depth at all times, as required by *CalME* to provide temperatures at all depths).

4.2.2 Subgrade Moisture Contents

Each track data logger in the 2000 NCAT Test also collected information provided by a time domain reflectometer (TDR) that was installed between adjacent experimental surface mixes. It was learned over the course of the study that subgrade moisture contents varied between 22 to 25 percent regardless of whether sections were built in cut or in fill areas (*7*). A later investigation (in sections built after the conclusion of the 2000 NCAT test) indicated that TDR measurements were approximately double the actual moisture contents. Extensive erosion at edge drain outlets (installed every 150 m) indicated that water was being transported along the side of the pavement structure, but it was not possible to determine whether the water was being removed from the pavement or simply infiltrating the drainage trench from soil along the shoulder.

No moisture data was provided on the NCAT website. Accordingly, no consideration for moisture change was made in this study.

4.3 Structure

Structure parameters include layer thicknesses and the mechanical properties of materials used in the pavements.

4.3.1 Layer Thickness

The layer buildups for all four selected sections were identical. Layer thicknesses are listed in Table 2.1.

4.3.2 Asphalt-Bound Layer Stiffness

Stiffness for asphalt-bound layers is defined by Equations (1) and (2), and in order to use the equations, it is necessary to determine the model parameters in these two equations.

These parameters can be determined from a set of frequency sweep tests using either a beam bending or a triaxial setup in the laboratory at temperatures that represent in-situ pavement conditions. Frequency sweep tests to measure dynamic modulus using triaxial tests were conducted at 64°C only in the 2000 NCAT Test. These tests do not provide enough information to define Equations (1) and (2), and UCPRC did not conduct further frequency sweep tests for this study.

Given the lack of frequency sweep test data, stiffness model parameters for all asphalt bound materials except ATPB were determined using the NCHRP 1-37A design guide ([*5*], Part II, Chapter 2), based on binder specification, aggregate gradation, air-void content, and asphalt binder content (i.e., at level 3 inputs).

The AC mix characteristics related to stiffness are listed in Table 4.3. These values are listed in Reference (*3*) except the ones for the AC bases, which are derived from report (*8*) for the 2003 NCAT Test. Aggregate gradation data needed to determine AC mix stiffness are listed in Table 4.4.

Table 4.3: AC Mix Characteristics

Mix Description	Binder PG Grading	Air Void (%)	Asphalt Content by Weight of Total Mix (%)	Bulk Specific Gravity of AC Mixture
N4 Surface	67-22	6.6	6.8	2.296
N6 Surface	67-22	5.6	6.8	2.270
N8 Surface	76-22	5.3	6.6	2.256
N9 Surface	76-22	5.5	6.7	2.279
AC upper base	76-22	6.0	4.27*	2.460
AC lower base	67-22	6.0	4.27*	2.460

*: These values are based on the report for the 2003 – 2006 NCAT Tests, assuming that the AC bases were designed to be the same.

Table 4.4: Selected Aggregate Gradation Data for AC Mixes Used in the Selected Sections

Mix Description	3/4"	3/8"	No. 4	No. 200
N4 Surface	100	91	68	6.0
N6 Surface	100	85	54	8.2
N8 Surface	100	85	55	7.5
N9 Surface	100	87	57	8.8
AC upper base*	94	72	53	5.1
AC lower base*	94	72	53	5.1

*: Values for these two mixes are based on the report for the 2003–2006 NCAT Tests, assuming that the AC bases were designed to be the same.

The NCHRP 1-37A guide requires the use of effective binder content by total volume. For AC surface mixtures, this is done by assuming that absorbed binder content is 1 percent of total mass. The actual equation for calculating effective binder content is:

$$V_{b,eff} = \frac{\frac{AC-1}{SG_b}}{\frac{100}{SG_{mix}}} \times 100 \qquad \textbf{(8)}$$

where AC is the binder content by weight of total mass, and
SG_b and SG_{mix} are specific gravities of binder and bulk AC mixture, respectively.

A value of 1.03 was assumed for SG_b. For AC base materials, Reference (*8*) provides effective binder content by mass; the effective binder content by volume was calculated accordingly.

After following the procedure outlined in the NCHRP 1-37A guide ([*5*], Part II, Chapter 2), model parameters for AC stiffness were obtained; these are listed in Table 4.5. Note that an error was found in the expression for β in Equation 2.2.4 in the design guide. The correct one should be:

$$\beta = -0.603313 - 0.393532 \times \log(\eta_{tr}) + \gamma \times \log(2\pi) \qquad \textbf{(9)}$$

This error was caused by the wrong conversion between loading time and frequency f=1/t. The correct relation is f=1/2πt, which is required to allow viscoelastic material to have roughly the same stiffness for the pairing loading time and frequency. Since Equation 2.2.4 in NCHRP 1-37A was merely a recast of Equation 2.2.3, all the regressions were conducted using the latter equation. The corrected Equation 2.2.4 should be used.

Table 4.5: AC Mix Stiffness Model Parameters for Use in *CalME*

Mix	δ	E_{ref} (MPa)	β	γ	aT	VTS	A
N4 Surface	0.69582	6160	-0.85194	0.313351	1.255882	-3.553	9.732517
N6 Surface	0.696707	6081	-0.85194	0.313351	1.255882	-3.553	9.732517
N8 Surface	0.713535	7498	-0.97762	0.313351	1.255882	-3.208	8.896086
N9 Surface	0.70983	7396	-0.97762	0.313351	1.255882	-3.208	8.896086
AC upper base	0.705747	8444	-0.97762	0.31335	1.255882	-3.208	8.89609
AC lower base	0.705747	7123	-0.85194	0.31335	1.255882	-3.553	9.73252
ATPB	2.477121	1199	0.39747	0.40000	1.256000	-3.554	9.74364

*: Reference moduli (E_{ref}) are given for loading time of 0.015 sec, and the reference temperature is 20°C.

AC mix stiffnesses, determined using the NCHRP 1-37A guide as shown above, were found to be inconsistent with the dynamic moduli measured in triaxial tests. Specifically, mix stiffnesses determined here were roughly 150 to 300 times larger than the ones measured in the triaxial tests. It is not clear what caused this discrepancy. At 64°C and frequencies from 0.1 to 10 Hz, the measured dynamic modulus ranged from 0.5 to 2.0 MPa, which is believed to be too low. By contrast, AC modulus predicted by the NCHRP 1-37A guide for the same conditions ranged from 100 to 600 MPa, which is believed to be more reasonable. It was therefore believed that the master curves for AC mix stiffness developed based on the NCHRP 1-37A guide are reasonable.

Table 4.5 also lists stiffness model parameters for ATPB. Such materials are quite different from normal AC surface layers in terms of aggregate gradation, binder content, and air-void contents. An attempt was made to use Tthe NCHRP 1-17A guide procedure to predict ATPB stiffness. However it was found that the predicted values were too low for ATPB materials (*9*). It was therefore decided to use the default values provided by *CalME*.

4.3.3 Unbound Layer Stiffness Model

Unbound materials, including aggregate base and subgrade, were treated as linear elastic materials with constant stiffness. No modulus test data were found available for the 2000 NCAT Test. However, extensive subgrade and aggregate base modulus tests were conducted in the 2003 NCAT Test (*8*). The subgrade materials used in the 2000 and 2003 tests were the same. It is assumed that the aggregate base material was also the same for the two research cycles.

The following discussions are based on results listed in the report for the 2003 NCAT Test (*8*).

Laboratory data indicated that subgrade resilient moduli were between 50 and 100 MPa, while aggregate base resilient moduli were either between 130 and 350 MPa (as tested by the material supplier) or between 30 and 70 MPa (as tested by ALDOT).

Backcalculation results from Falling Weight Deflectometer testing indicated that subgrade moduli were between 140 and 210 MPa for both the 2000 and 2003 NCAT Tests. Granular base moduli were believed to be between 35 and 100 MPa.

In summary, the subgrade moduli range from 50 to 210 MPa, while the aggregate base moduli range from 30 to 350 MPa. These ranges are relatively large but are nevertheless reasonable because of construction variability since they were measured at different locations. It was decided to use the average values of 130 MPa for subgrade and 190 MPa for aggregate base. A sensitivity study was conducted to make sure using these average stiffnesses for subgrade and aggregate base did not lead to significant error.

4.3.4 Asphalt-Bound Material Rutting Model Parameters

Rutting model parameters for the surface experimental mixtures were determined using data from RSST-CH tests conducted by UCPRC. This was done by minimizing the root mean square error between predicted and measured inelastic strain in RSST-CH tests. The inelastic strain model is shown Equation (10). The RSST-CH test data for the NCAT sections are stored in a comprehensive database maintained by Lorina Popescu. An *Excel* workbook was developed by Per Ullidtz using the "Solver" function to both import the shear test data and perform the minimization.

Six RSST-CH tests were conducted for each experimental mixture, with two levels of temperatures (45°C and 55°C) and three replicates. Since only one stress level (0.130 MPa) was used in the test, model parameter β

could not be determined. It was decided, therefore, to use instead the default value of 1.03, recommended by Reference (*14*). Furthermore, the reference shear stress τ_{ref} was set to 0.1 MPa (the default value in *CalME*).

To compare the fitted permanent shear strain with the measured ones, a normalized permanent shear strain $\gamma^i_{normalized}$ defined below was used:

$$\gamma^i_{normalized} = \ln\left(\gamma^i \Big/ \exp\left(\beta \times \tau \Big/ \tau_{ref} \right) \times \gamma^e \right) \quad \textbf{(10)}$$

in which the variables are the same as defined in Equation (5). A comparison of calculated and measured normalized permanent shear strain for different surface AC mixes is given in Table 4.6.

Rutting model parameters for the two AC base materials could not be determined from laboratory test data because no RSST-CH tests were done using those materials. Rutting model parameters for the upper AC base were assumed to be the same as for the N9 surface mix, and the ones for AC lower base were assumed to be the same as for the N6 surface mix.

Table 4.6: AC Surface Mixes Rutting Model Parameters for Use in *CalME*

Mix	Type	A	α	τ_{ref} (MPa)	β	γ	K*
N4 Surface	"g"	-0.40697	3.2263	0.1	1.03	2.123352	1.4
N6 Surface	"g"	-0.33868	3.2217	0.1	1.03	2.37106	1.4
N8 Surface	"g"	-1.66239	4.6995	0.1	1.03	2.83013	1.4
N9 Surface	"g"	-0.95491	3.3893	0.1	1.03	1.99385	1.4
AC Upper Base	Same as "N9 Surface" mix						
AC Lower Base	Same as "N6 Surface" mix						

*: *K* is the shift factor that needs to be adjusted as part of the calibration process so that the calculated rut can match the measured values.

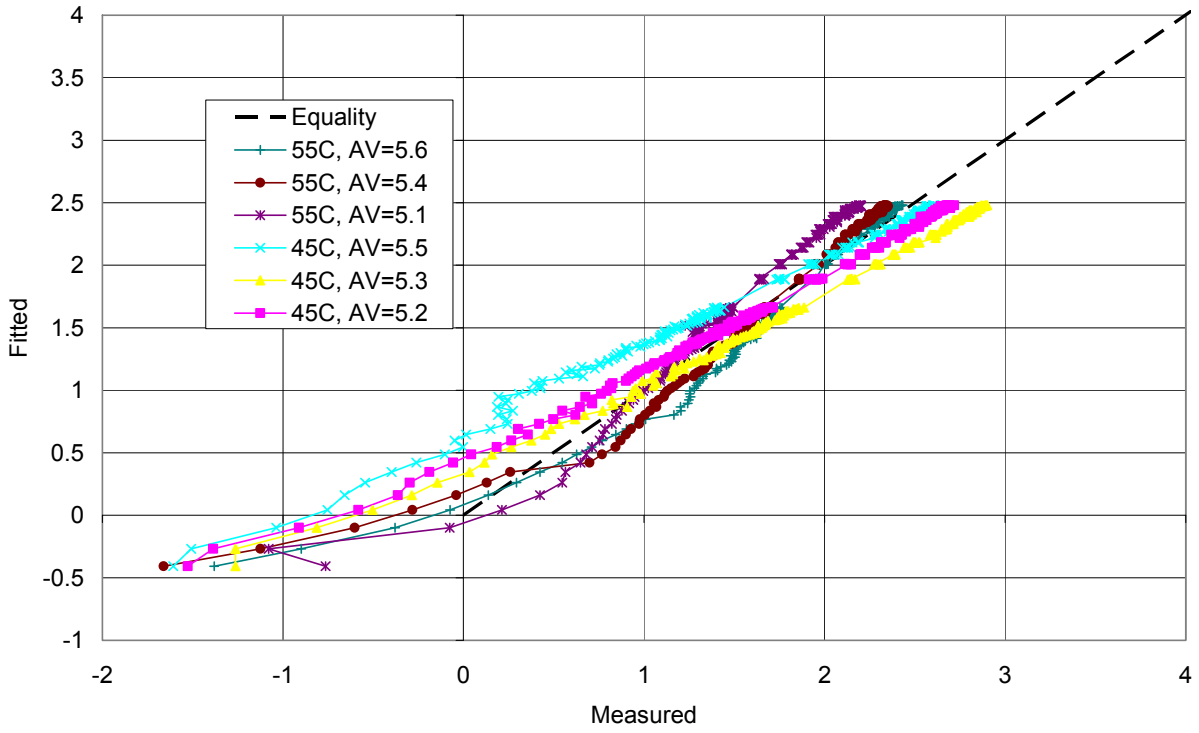

Figure 4.4: Comparison of fitted and measured normalized permanent shear strain from RSST-CH test results for N4 surface AC mix.

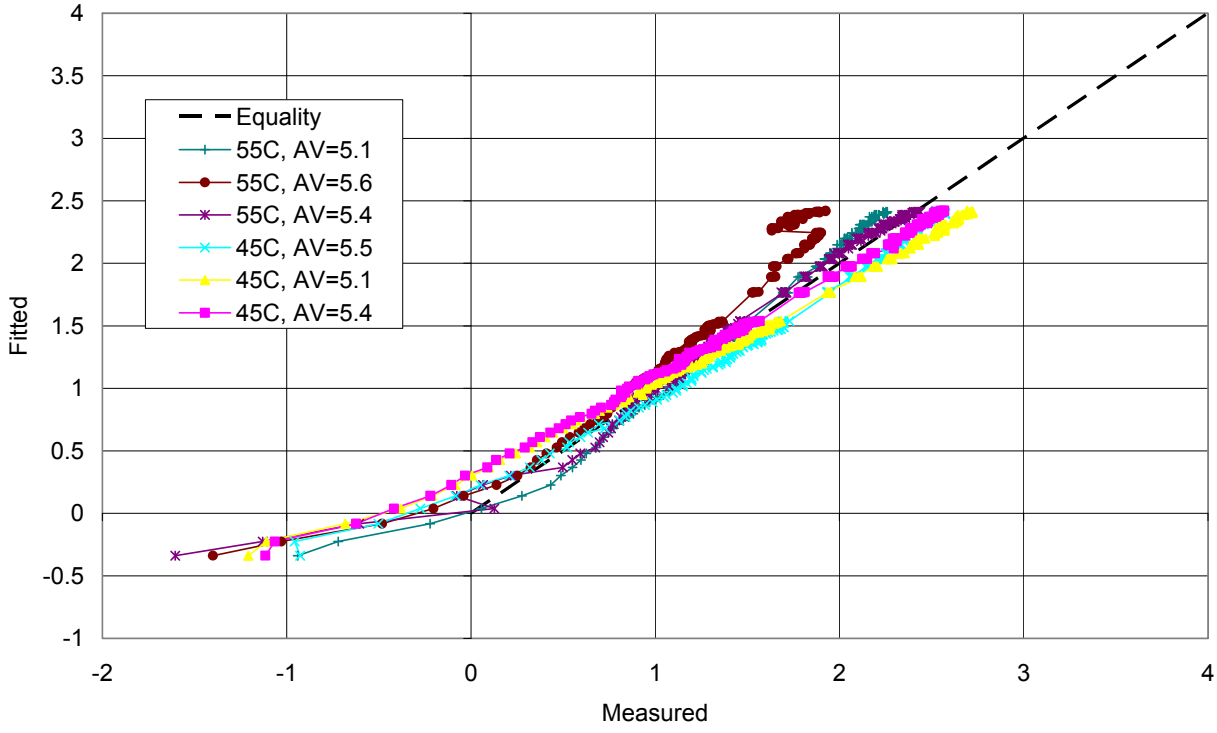

Figure 4.5: Comparison of fitted and measured normalized permanent shear strain from RSST-CH test results for N6 surface AC mix.

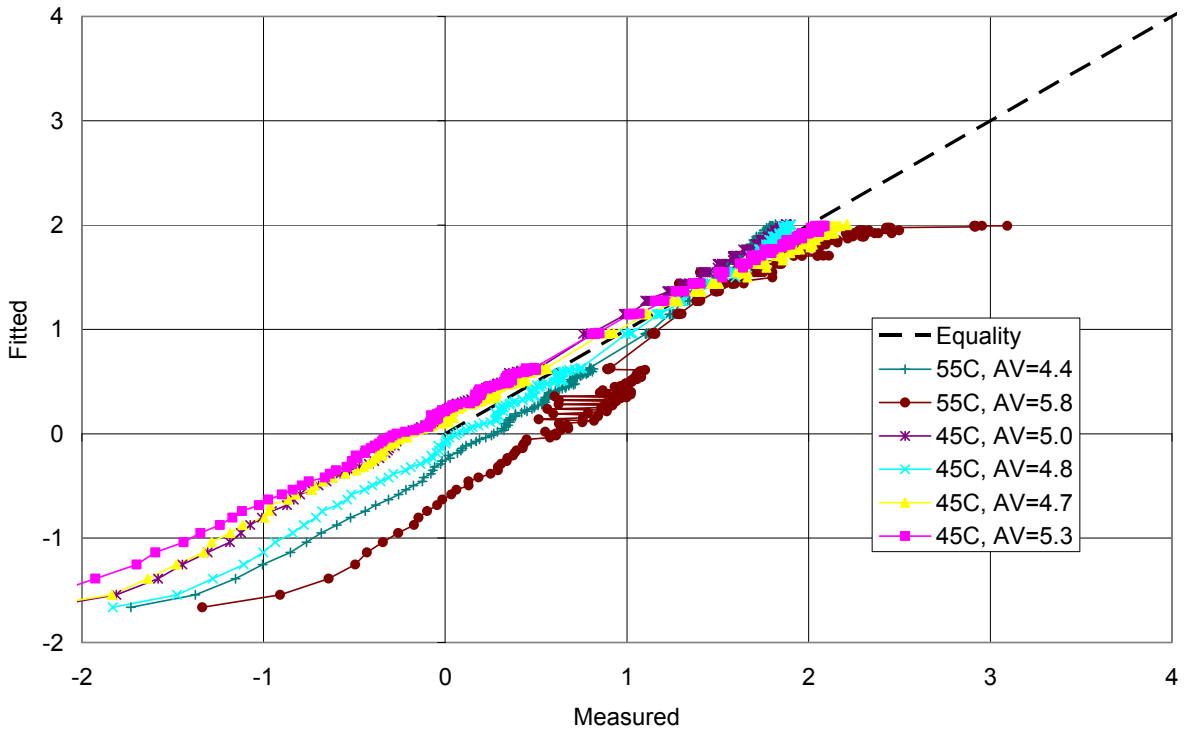

Figure 4.6: Comparison of fitted and measured normalized permanent shear strain from RSST-CH test results for N8 surface AC mix.

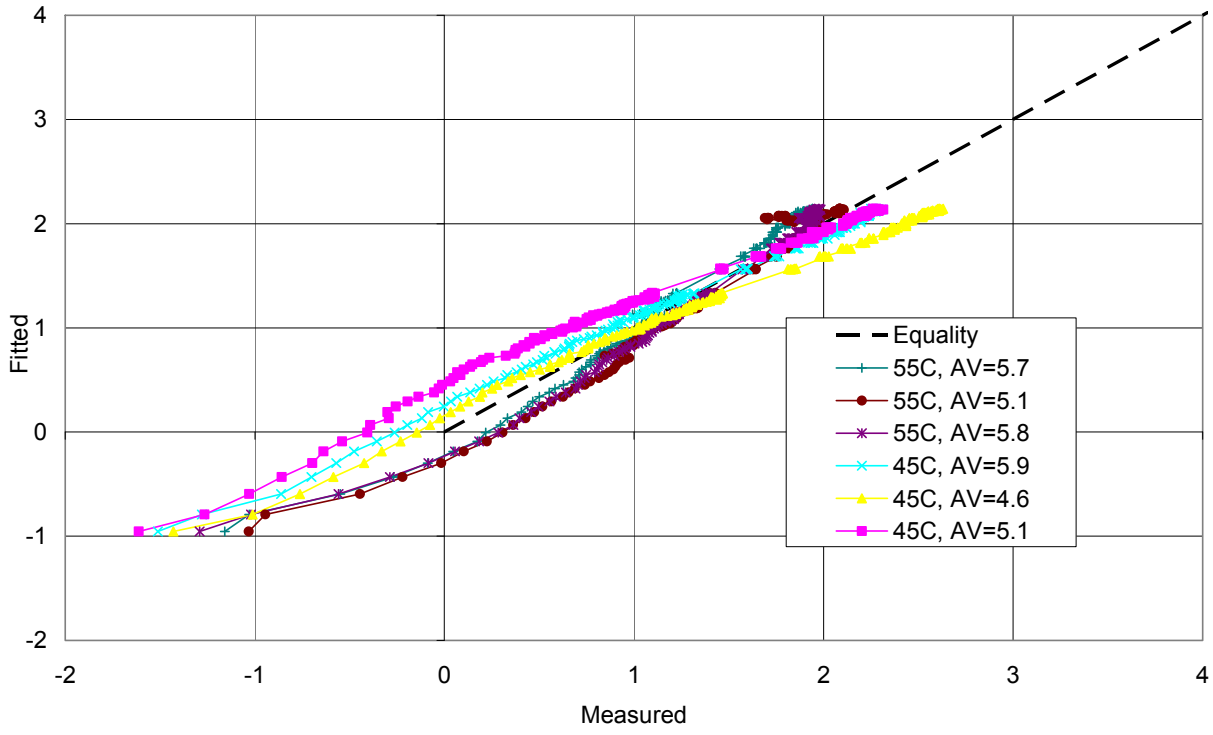

Figure 4.7: Comparison of fitted and measured normalized permanent shear strain from RSST-CH test results for N9 surface AC mix.

Rutting model parameters for the ATPB layer were taken from the default *CalME* material library for material named "ATPB-AC." Specifically, the parameters are listed below:

Type: "t", A*K=7, $\alpha = 0.2$, $\tau_{ref} = 0.1$ MPa, $\beta = 1.03$, $\gamma = 1.0$

4.3.5 Rutting Model Parameters for Unbound Layers

Rutting model parameters for aggregate base and subgrade were taken from the default *CalME* material library for materials named "AB" and "Clay." The actual values are listed in Table 4.7. These are generic rutting material properties that are the same for all aggregate base and clayey soils respectively.

Table 4.7: Unbound Material Rutting Model Parameters for Use in *CalME*

Mix	Type	A	α	ε_{ref} (ue)	β	E_{ref} (MPa)	γ
Aggregate Base	"e"	0.8	0.333	1000	1.333	40	0.333
Subgrade	"e"	1.1	0.333	1000	1.333	40	0.333

4.4 Traffic

A total of 10 million ESALs of traffic were applied over a two-year period. Limited truck traffic began on the new pavements on September 19, 2000, and authorization for full fleet operations was granted on November 19, 2000. Traffic operations were completed on the 2000 Track at approximately 2 p.m. on December 17, 2002.

The ESALs were applied with four fully loaded trucks with three trailers per tractor. Each tractor pulled a load of approximately 152,000 pounds: 20,000 for each of seven loaded axles and approximately 12,000 pounds for the front steering axle. The first two axles actually formed a tandem axle but were treated as two single axles in the study, following the convention used in the WesTrack test (*11*). These trucks were the same as the ones used in the WesTrack test previously operated at the Nevada Automotive Test Center. The truck is shown in Figure 4.8. Each pass of the triple-trailer truck applied 10.48 ESALs of traffic (p. 25 in [*11*]).

Generally, trucking operations ran from 5 a.m. to approximately 11 p.m., with about an hour of downtime midday to accommodate refueling and driver shift changes. Truck computers were set such that cruise speed was held constant at 72 km/h (44.7 mph), which is the design speed of the test oval.

Daily accumulated ESAL counts for the 2000 NCAT Test are stored in the table ESALS_2000 on the NCAT database. *CalME* applies traffic in terms of axle counts rather than ESALs. Accordingly, the daily truck counts were calculated based on the ESAL record. The daily truck counts were then further divided evenly into hourly truck counts, assuming the daily trucking stopped from 1:30 p.m. to 2:30 p.m.

Figure 4.8: Triple trailer truck used to apply trafficking.

The truck tire pressure was 690 kPa (*12*), and the on-center distance between the two dual wheels was assumed to be 300 mm based on data for WesTrack, which also used triple trailers to apply trafficking. The 300 mm distance had to be assumed because no relevant reference could be found in NCAT reports. The truck wheel wander pattern in NCAT tests was described in (*13*) for the 2003 NCAT Test. It was assumed that the wander pattern for the 2000 NCAT Test was the same as in the 2003 NCAT Test. According to the report (*13*), truck wander follows a normal distribution with standard deviations of 225 mm for the morning shift and 193 mm for the afternoon shift. A statistical summary of the wander pattern is shown in Figure 4.9. It was therefore decided to use a standard deviation of 210 mm, the average of the morning and afternoon shifts, in *CalME* simulations in this study.

A small *Matlab* routine was written to transfer the hourly truck-loading schedule into the *CalME* project database.

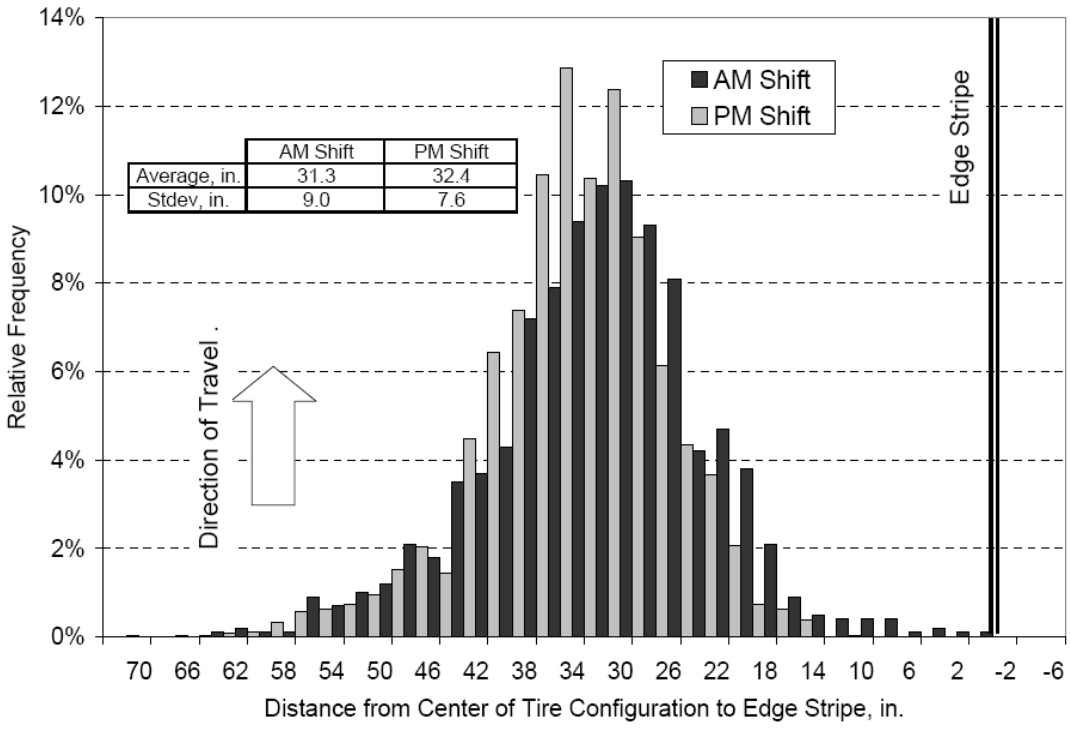

Figure 4.9: Statistical summary of wheel wander data for the 2003 NCAT Test.

4.5 Performance

Truck trafficking was stopped every Monday to conduct a pavement condition survey and run necessary tests for monitoring pavement performance. The 2000 NCAT Test was intended to serve primarily as a rutting experiment. As anticipated, rutting was the most notable surface distress observed in the research portion of all sections at the completion of truck traffic; however, most rut depths were relatively shallow.

Rutting measurements were taken on the middle 45 m of each section's 60 m length. That middle research portion of each test section was further divided into three 15 m measurement replicates, each containing a randomly located transverse profile across which elevations were measured each week.

4.5.1 Rutting Measurement Methods

Rutting was measured with three methods in the 2000 NCAT Test. The data processing was conducted by the NCAT research team.

These methods are listed below:

- **Rutting via three-point approximations using a high-speed laser profiler van:** The high-speed approach characterized each section with a single number that represented the average rut depth of the entire 45-m research length. The three-laser approach in the high-speed system reports a single rut depth as the average difference in vertical elevation between the wheelpaths and the midlane pavement surface. Because this method is not capable of considering rutting geometry outside the wheelpaths, it was expected that transverse profiles would be needed to serve as the primary source of information as shear outside the wheelpaths became more influential.
- **Rutting via precision level profiles:** A precision level (known commercially as a "Dipstick") was walked across each of three stratified random locations within each section every Monday. Two algorithms can be used to estimate rut depth from weekly surface elevation measurements using geometries that either include (i.e., 6-point) or ignore the contribution of elevations at the outer edges of both wheelpaths (i.e., 3-point). In the 6-point approach, the three elevations that define the peaks and valley of the left wheelpath are used to compute a maximum trough depth for the left wheelpath. The same procedure is used to produce a maximum trough depth for the right wheelpath, which is then used to compute a single average rut depth for the entire transverse profile.
- **Rutting via wire line:** After traffic operations had been completed (i.e., all 10 million ESALs had been applied), it was possible to invest the time necessary to measure rut depths using more traditional methods, such as a wire line. Three of the nine measurement locations were the same as those used in weekly tests, while the other six locations were spaced evenly over the remaining longitudinal length of each test section.

The 3-point and 6-point final rutting results, measured using a precision level, were compared with the ones measured with a wire line, as shown in Figure 4.10. The figure clearly demonstrates the superiority of the 6-point algorithm in comparison to the 3-point method. As a result of this observation, it was determined that the 6-point method would be used to quantify weekly rutting performance throughout the two-year traffic cycle. Final wire line values were then used to calibrate the entire record of weekly 6-point (profile-based) rut depths by computing the ratio of final wire-based to final profile-based values for each experimental section. This effort generated a **constant multiplier for each test section** that was then used to correct 6-point rut depths measured at all times, theoretically making them equal to wire line measurements.

Next, the total change in rut depth that had occurred at the time each weekly measurement was made (induced rutting) was computed for each section. Induced rutting values can differ slightly from measured rutting values by the amount of apparent rutting that existed before any traffic was applied. Slight surface irregularities (e.g., roller marks) can actually produce negative geometric rutting at zero traffic, which leads to a total traffic-induced rutting that is more (or less) than the measured wire line value. To account for this effect and eliminate the bias it would induce both on field comparisons and on laboratory predictions, it is necessary to **use the original negative rut as the starting point** for section deformation instead of zero.

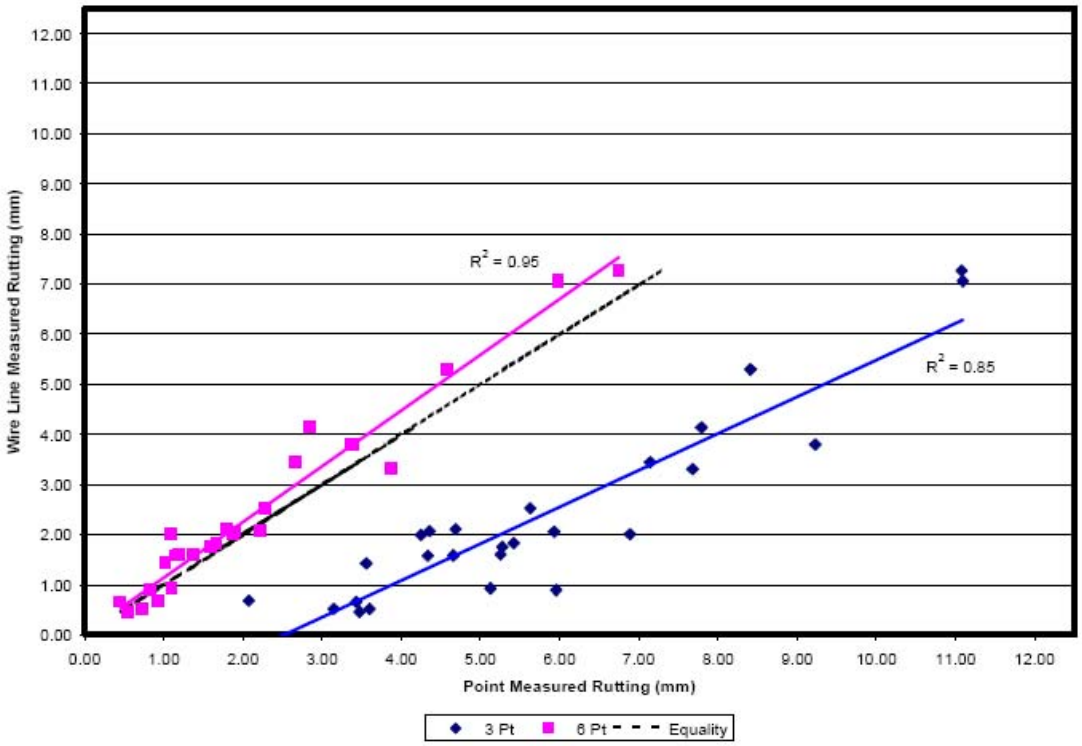

Figure 4.10: Graphic comparison of final 3-point and 6-point rutting versus final wire line rutting.

The weekly change in rutting was visually best fit to produce a single, smooth progression of induced rutting over the life of the two-year project. It was necessary to smooth the data in this manner to prevent apparent negative changes in induced rutting (resulting from experimental error). **The final product of this effort** was a record of incremental rutting for each measurement interval. Any apparent rut depths that existed before traffic was applied were not included. Also, the reporting dates for rutting results were selected to represent points in time between which rutting progressed more or less constantly.

The final processed data are saved in the NCAT database in the table named "DIP_2000." The rut depth developments are shown for the selected sections in Figure 4.11. The rutting data were prepared and saved in the *CalME* database in the table "ProjectRutting" so that the simulation results could be compared directly against measured values.

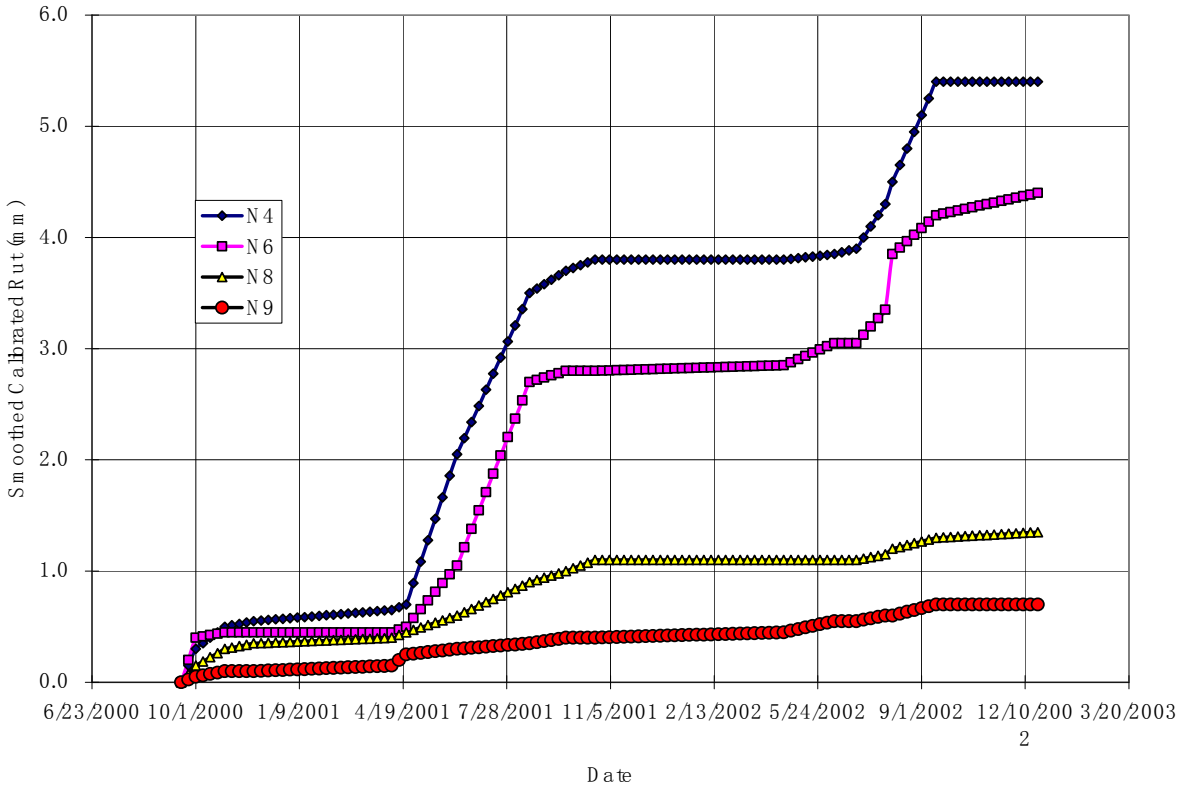

Figure 4.11: Rutting of selected sections obtained after data processing.

4.5.2 Other Performances

The same three-laser high-speed profiler that estimated 3-point rut depths was also equipped with an inertial compensation system to normalize vehicle dynamics and produce profile-based roughness measurements for each section. Output data were summarized in 8 m increments such that the middle 46 m of each section could

be examined without the influence of adjacent transverse joints (affecting approximately 8 m on both ends of each section). Roughness was reported in m/km in accordance with the International Roughness Index (IRI) approach, which is a mathematical assessment of amplified profile wavelengths tuned specifically to quantify a roadway's feel for a traveler in a passenger car.

Additionally, the laser mounted in the right wheelpath sampled data at a relatively high frequency (64 kHz). This allowed the onboard software to quantify the macrotexture of each experimental pavement by digitizing the rapid vertical distance measurements (read at an accelerated rate of three samples per millimeter at test track speeds). *Macrotexture* is a term used to define short (0.5 to 50 mm) wavelength irregularities in the surface of a pavement, and is a function of the gradation of the aggregates in the mix, void structure, and the like. Wavelengths shorter than 0.5 mm are thought to represent the surface texture of the aggregate itself, which is referred to as *microtexture.* Wavelengths greater than 50 mm but less than 60 m are not indicative of texture but do contribute to roadway roughness felt by the motoring public.

Cores were cut every three months from the last 7.5 m of each section so that densification of individual lifts could be quantified. Both nuclear and non-nuclear density testing was performed on the spot where the core would be taken to also facilitate density gauge correction each time coring was conducted. Subsequent testing with both nuclear and non-nuclear devices could then be conducted within the section in the wheelpaths at stratified random locations. In this manner, densification within the research portion of each section could be monitored each week in a nondestructive manner.

Calibration of IRI performance is not the focus of this study.

5 RUNNING *CalME*

This chapter describes some of the key details for running *CalME* and performing model calibration. Note that these discussions may become obsolete in future versions of *CalME*.

5.1 Mode of *CalME* Analysis

CalME can be run in various modes that determine how the user specifies model inputs and performance data. The running mode is determined by value of the "HVS" field in the "ProjectLayer" table. A "0" for all layers indicates routine pavement design, a "1" indicates HVS tests, and a "2" or any other larger number indicates track tests (e.g., NCAT Test Track, WesTrack).

To run *CalME* in track test mode, the user first needs to create a new project for routine pavement design and then must modify the "HVS" field manually in the "ProjectLayer" table for the project. In this study, the "HVS" field was set to 3 for all the projects, indicating that these projects represent track tests.

For track test simulations, *CalME* reads temperature records and loading schedules from tables that are different from the ones used for routine pavement design. These special tables are listed in Table 5.1. These tables need to be populated properly when *CalME* is directed to run in Track Test mode.

Table 5.1: Tables Used for Track Test Simulation in *CalME*

Table Name	Description
TrackNames	Relates the "HVS" field in the "ProjectLayer" table to the name of the test track and the name of the temperature data set, and one record for each "HVS" field value; different "HVS" field values can correspond to the same track name.
TrackWheels	Provides information on various types of axles used in a specific track test; axle parameters include number of wheels, tire pressure, wander settings (offset and standard deviation), and tire distance; these settings are shared by all the test sections for a test track.
TrackLoads	Defines the trafficking schedule for a given track; schedules are given in hour intervals with parameters that include number of passes for each axle and load applied by each axle
TrackTemperatureDepths	Provides depths at which temperature data are provided, one record for each test track.
TrackTemperatures	Provides hourly pavement temperatures for a given temperature data set and track name.

5.2 Parameters to be Calibrated

Parameters that can be adjusted to match calculated rut with measured rut include:

- Shift factor "K" for the rutting model: This parameter relates performance predicted by laboratory models to the ones measured in the actual pavement. "K" value can be set to various values for different test sections during calibration, but one constant value is needed to simplify routine design.
- Amount of initial rutting removed by M&R (Maintenance and Rehabilitation) activities: This is necessary because the measured rut was forced to start from zero by the NCAT research team. This value is set through the menu "Parameters"-> "Set dRut, dIRI" and can be different for each test section. Note that *CalME* simply subtracts the specified amount of rut from the calculated results.

6 RESULTS AND DISCUSSION

6.1 Introduction

This chapter presents the results obtained in the calibration study, including sensitivity of the β parameter for the AC rutting model, sensitivity of unbound layer stiffness and wander pattern, comparisons of measured and calculated rutting performance, and discussions on the validity of models used in *CalME*. As mentioned in the previous chapter, assumptions had to be made with respect to several inputs due to lack of data. The sensitivity studies presented here are used to evaluate the amount of error introduced by these assumptions.

In the sensitivity studies listed below, Section N4 was always used. There was no wander allowed to make simulations run faster, and the "Linear Elastic Theory" option was checked as the strain calculation engine. In the actual simulation, wander *was* allowed.

6.2 Sensitivity of the β Parameter for the AC Rutting Model

As mentioned in Section 4.3.4, the β parameter for the AC rutting model cannot be determined in this study because RSST-CH tests were conducted at only one stress level. Although a value of 1.03 has been used in the past for calibrations using HVS and WesTrack data (*1*), other value ranges from 0 to 0.5 have been found where RSST-CH tests were conducted at different stress levels. Specifically, laboratory results obtained in Strategic Plan Element 4.10 (i.e., Development of Improved Rehabilitation Designs for Reflection Cracking) indicate that β was approximately 0.5 for DGAC with AR4000 binder, and approximately 0.0 for gap-graded mix with rubber-modified binders. It is therefore necessary to evaluate the sensitivity of calculated rutting performance with respect to different values for β.

Five sets of rutting model parameters were determined for the surface AC in Section N4, using the same RSST-CH data. These parameters are listed in Table 6.1. The five sets of parameters fit the RSST-CH data with roughly the same amount of RMS.

The calculated ruts corresponding to three different given β values are shown in Figure 6.1. Apparently, the calculated ruts are roughly in proportion to each other. Figure 6.2 shows the relation between "Ratio of Calculated Rut" and the value for β parameter. Ratio of Calculated Rut is obtained by dividing the calculated rut at a certain load repetition for a certain given β value by the corresponding value for β=1.03. As shown in Figure 6.2, a simple linear regression fits the relation very well. As β increases, calculated rut increases, too. When β changed from 1.03 to 0.0, the calculated rut decreased by about 35 percent. Although this change is not small, it is not regarded as significant enough to justify using a value different than 1.03, without support from additional laboratory test data. The original value of 1.03 was determined based on data from the WesTrack study (*14*).

With the linear relation between β and the calculated rut by *CalME* shown in Figure 6.2, it is easy to get results for different β value once its recommended value has been finalized with the support of sufficient RSST-CH test data. The shift factor can then be adjusted accordingly if necessary. For example, a β value of 0.5 corresponds to a ratio 0.83 for calculated rut. This implies that if a β value of 0.5 were used instead of 1.03, all the rut results calculated by *CalME* must be multiplied by 0.83.

Table 6.1: Rutting Model Parameters for N4 Surface Mix with Different β

Mix	Type	A	α	τ_{ref} (MPa)	β	γ	K
N4 Surface	"g"	-0.40697	3.2263	0.1	1.03	2.123352	1.4
N4 Surface	"g"	1.10678	2.7900	0.1	0.00	1.918673	1.4
N4 Surface	"g"	0.37447	3.0833	0.1	0.50	2.108861	1.4
N4 Surface	"g"	0.74236	3.0172	0.1	0.25	2.101845	1.4
N4 Surface	"g"	0.00608	3.1504	0.1	0.75	2.115838	1.4

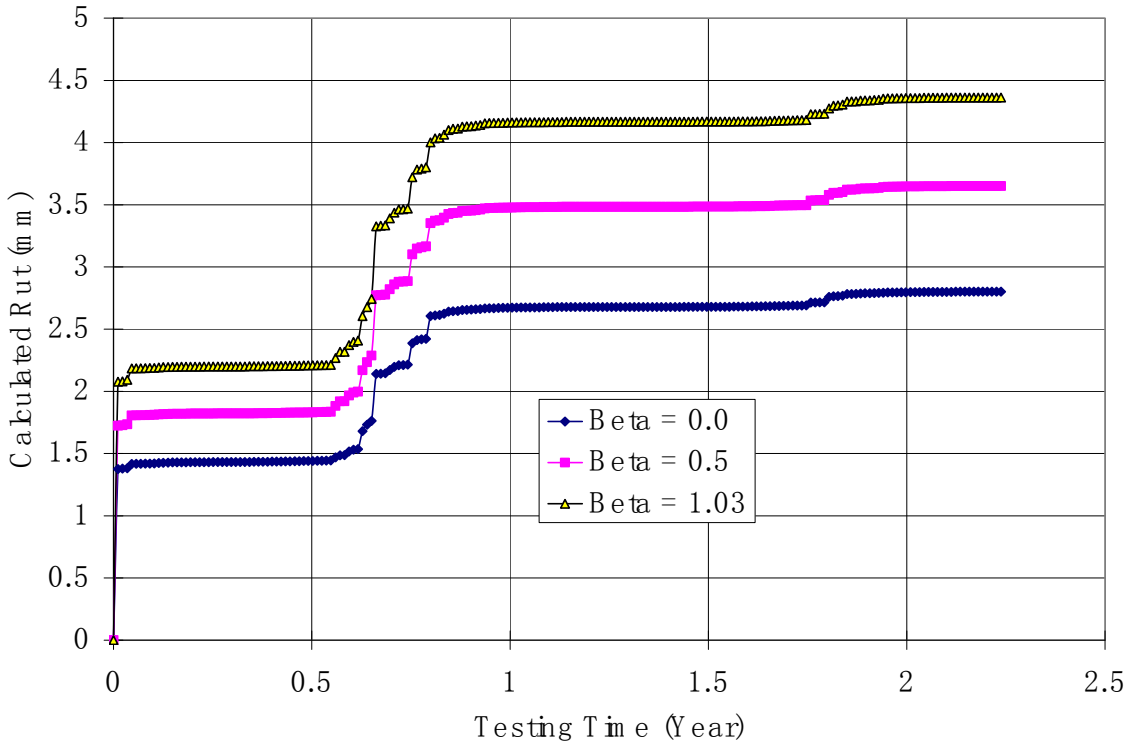

Figure 6.1: Effect of β parameter in AC rutting model on calculated rut.
(Note: changing β results in changes in other parameters in order to fit the same RSST-CH test data.)

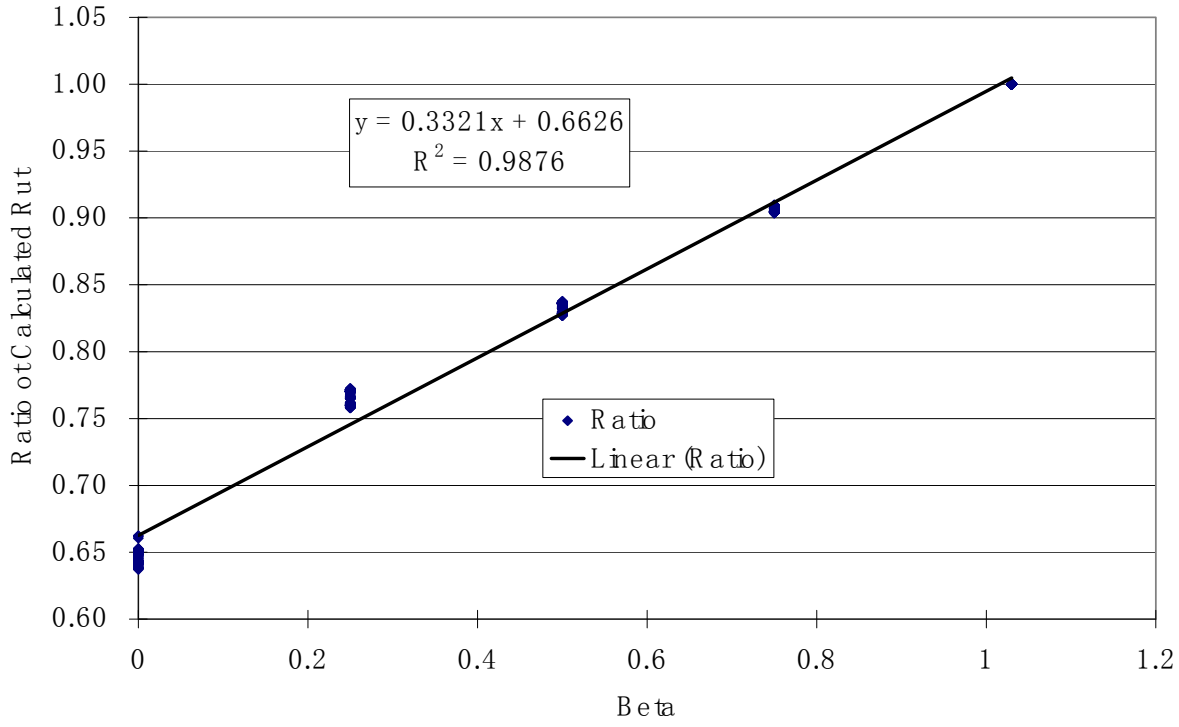

Figure 6.2: Ratio of total rut compared to values when β=1.03.

6.3 Sensitivity of Aggregate Base Stiffness

As mentioned in Section 4.3.3, unbound layer stiffness was found to vary over a fairly large range. Since only the midrange values for both aggregate base and subgrade were used in the simulation, it proved necessary to evaluate the sensitivity of surface rutting on variations of unbound layer stiffness. This was done by comparing the calculated rutting results for Section N4 with various aggregate base stiffnesses. Specifically, aggregate base stiffness was set to 30, 190, and 350 MPa, respectively. The resulting calculated rutting histories are shown in Figure 6.3.

When running the sensitivity analysis, no wander was allowed, and the dRut parameter was set to 1.5 mm, based on preliminary simulations. As shown in Figure 6.3, the differences between rutting results are quite small. The final ruts are 3.0, 2.9, and 2.8 mm for aggregate base stiffnesses of 30, 190, and 350 MPa, respectively. Accordingly, the maximum error caused by using a midrange value (190 MPa) is: 0.1/2.9*100% = 3.5%. This error is regarded as minimal.

6.4 Sensitivity of Subgrade Stiffness

Sensitivity analysis of subgrade stiffness was conducted similarly to the analysis of aggregate base stiffness. The calculated rut for different subgrade stiffnesses is shown in Figure 6.4. As shown in the figure, the differences in calculated ruts are minimal, and using midrange value for subgrade stiffness is regarded as sufficiently accurate. Note that rut depth is not sensitive to subgrade stiffness in this particular case because the structure is too strong and not because subgrade stiffness is not important in general.

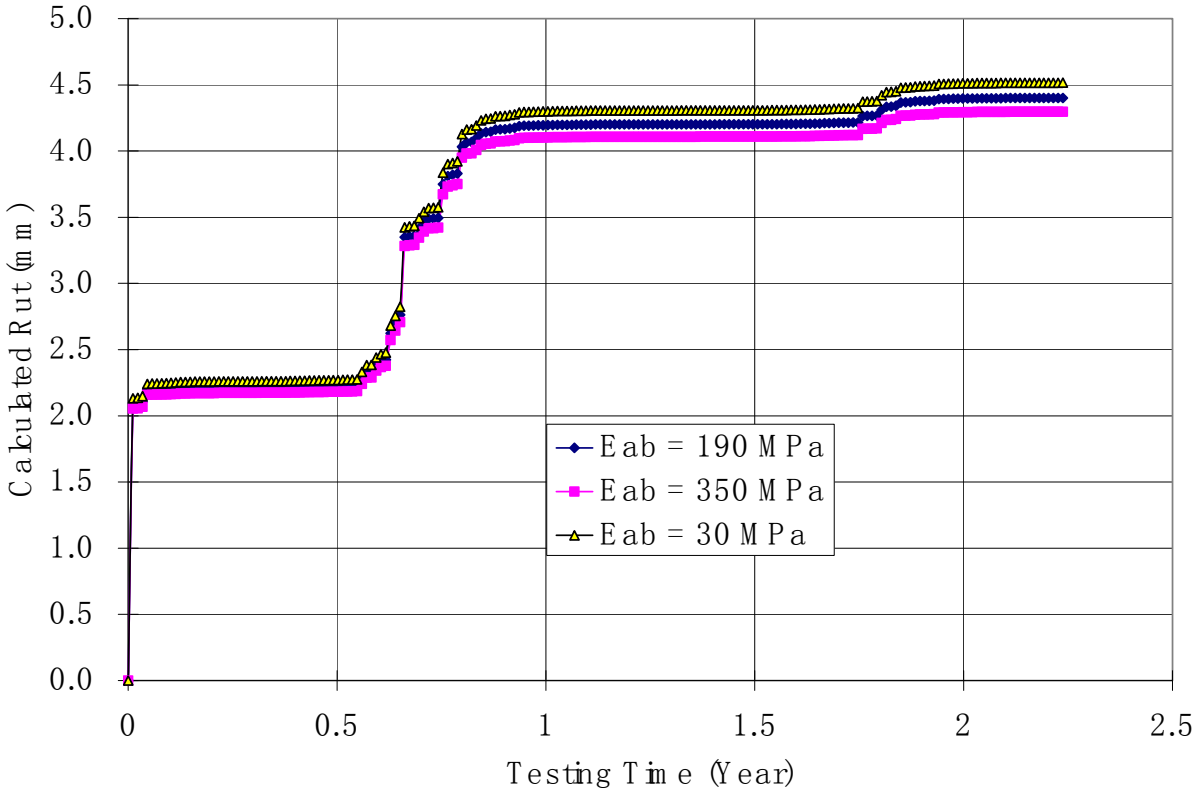

Figure 6.3: Effect of aggregate base stiffness on calculated rut.

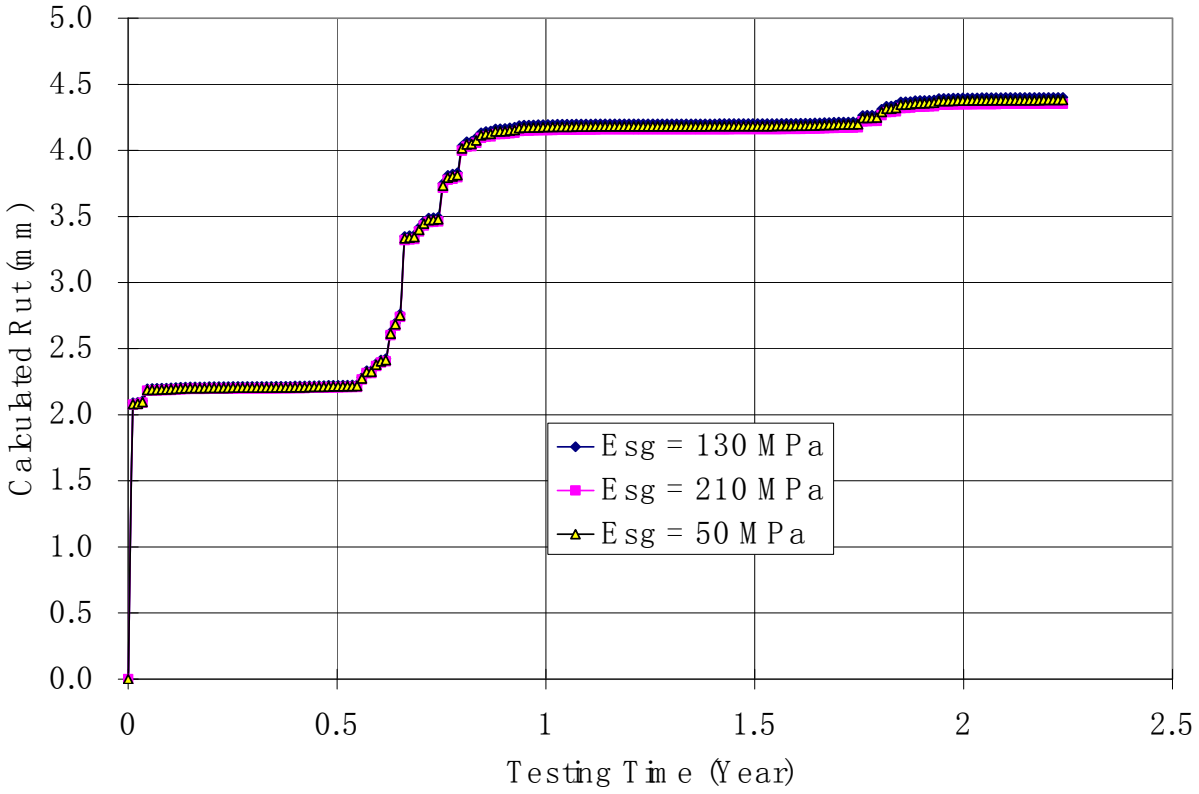

Figure 6.4: Effect of subgrade stiffness on calculated rut.

6.5 Effect of Wander

Checking the "wander" option in *CalME* leads to a significant increase in simulation time. It would be helpful to know whether this additional time is actually necessary.

CalME has a default wander pattern with normal distribution for wheel positions and a standard deviation of 300 mm for wheel offsets. The traffic in the NCAT Test followed a normal wander pattern, with standard deviations of 210 mm for wheel offsets.

CalME simulations were run with three wander settings: (1) no wander, (2) default wander pattern in *CalME*. (3) NCAT Test wander pattern. The resulting rutting development plots are shown in Figure 6.5, which demonstrates that rut develops significantly faster when there is no wander in the traffic compared to the case when there *is* wander. The difference in calculated ruts between the two wander patterns is very small, however, and can be ignored.

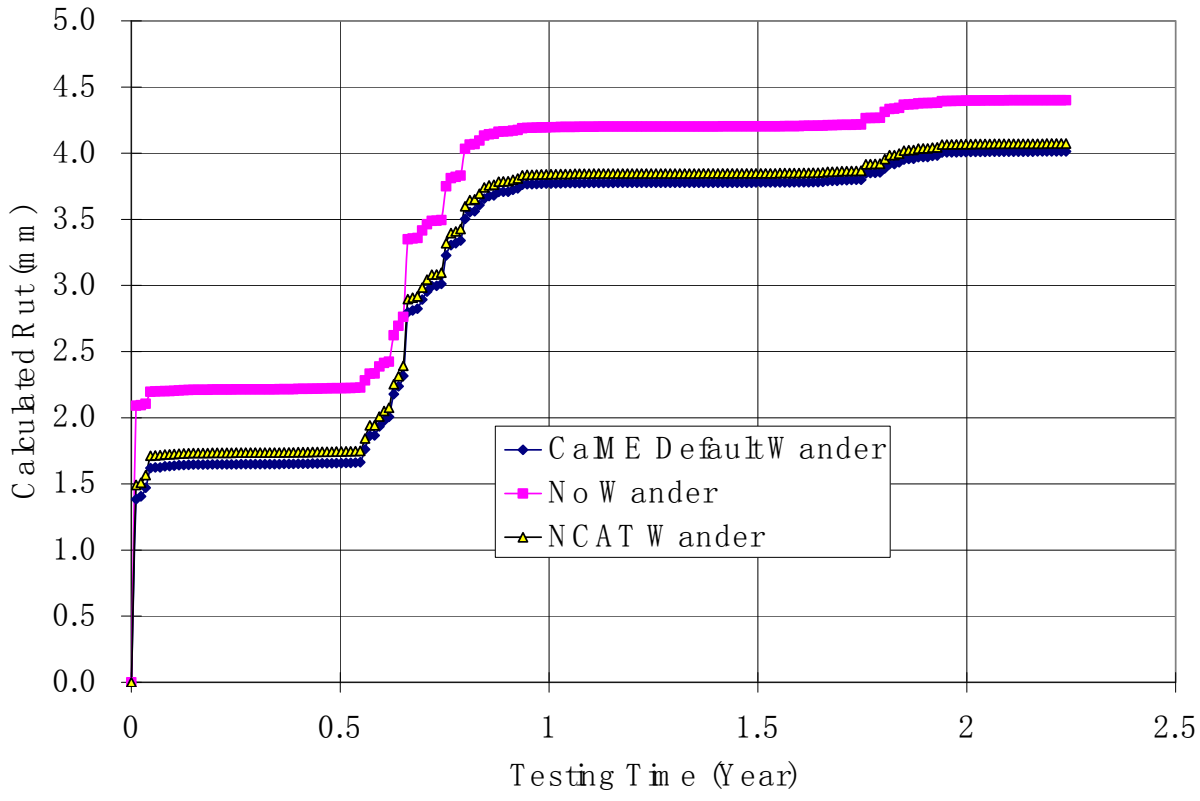

Figure 6.5: Effect of wander pattern on calculated rut.

6.6 Contribution to Rutting from Different Layers

Compression calculated for each layer in Section N4 when no wander was allowed is shown in Figure 6.6. The sum of compression in each layer is equal to the total downward rut calculated by *CalME* plus the dRut value. As shown in the figure, most of the compression (95 percent in this case) occurs in the surface AC layer. The underlying AC layers (upper and lower AC base, ATPB) recorded no compression at all because they were below 100 mm (3.9 in.) depth.

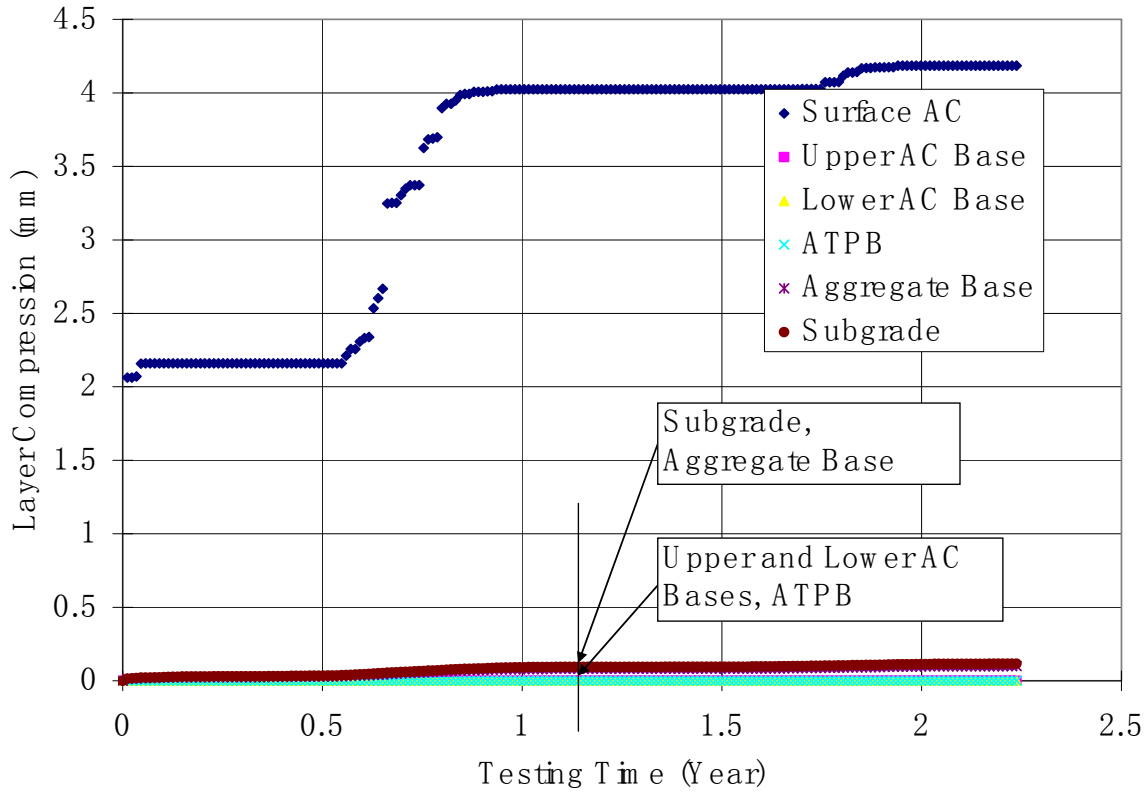

Figure 6.6: Compression in each layer for Section N4, no wander allowed.

6.7 Comparison between Calculated and Measured Rutting

Ruttings calculated by *CalME* are maximum downward permanent deformations. However, measured surface rutting in the 2000 NCAT Test were total ruts, i.e., the absolute sum of both upward and downward deformations. The ratio between downward rut and total rut was found to range mostly between 0.6 and 0.8, based on results in HVS tests conducted by UCPRC. Accordingly, the calculated rutting results should be close to measured values but cannot be compared directly with such values. By contrast, the trends for calculated rutting should be the same as those for measured values.

The uncorrected calculated ruts are shown in Figure 6.7. Qualitatively, these calculated results match well with the measured rutting performance as shown in Figure 4.11. Specifically, the two figures both show that:

- The relative ranking for rutting performance is from best to worst: N9, N8, N6, N4.
- The modified binders (with PG 76-22 binder) have significantly smaller amounts of rutting than the unmodified binders (with PG 67-22 binder).
- Rut increases quickly during summer time (April to August), but remains roughly unchanged during the rest of the year.
- Much more rutting occurred in the first summer than the second summer.
- The final rutting amounts have the same order of magnitude.

The close match between calculated and measured rut makes it reasonable to calibrate the *CalME* rutting model.

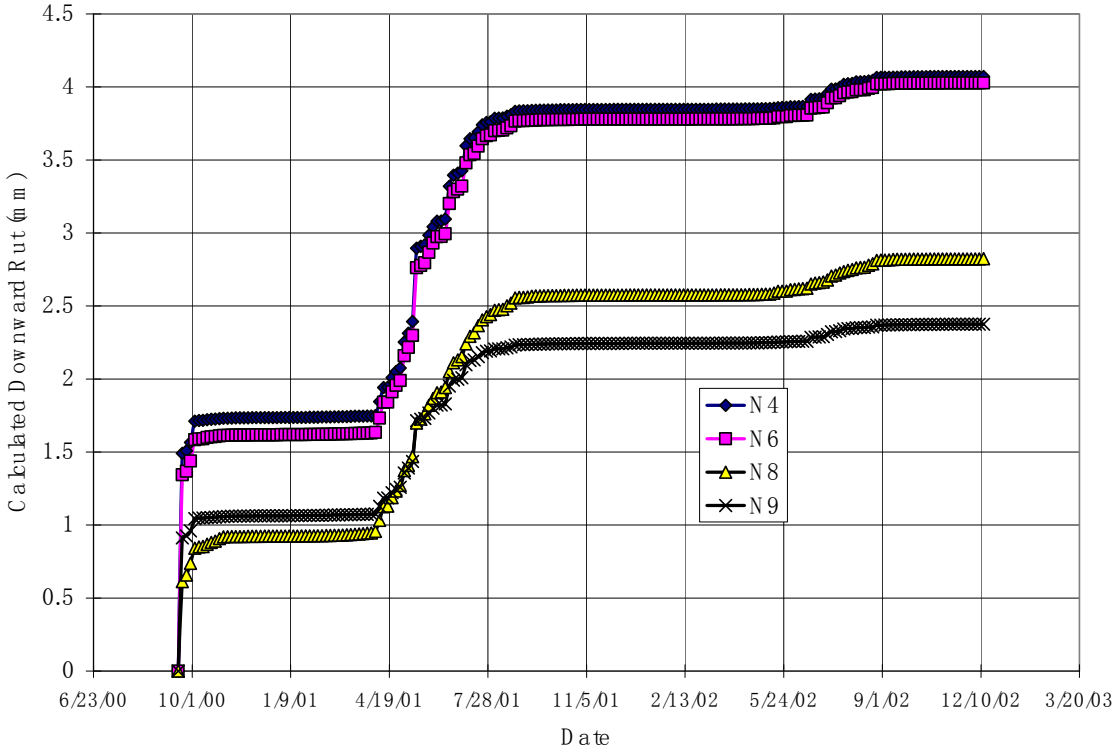

Figure 6.7: Calculated downward rut, with dRut set to zero for all sections.

6.8 Calibration of dRut and *K* Value for Individual Sections

As discussed in Section 6.7, the calculated ruts are downward permanent deformations and need to be divided by a value between 0.6 and 0.8 before they can be directly compared with measured values. As discussed in Section 5.2, two parameters can be adjusted: *K* and dRut. *K* was set to 1.4 when obtaining the results shown in Figure 6.7, while dRut was set to 0. Note that the purpose of Figure 6.7 was to show whether there is a reasonable match between the *CalME* predictions and the actual measurements.

The calibration can be done using the *Excel* solver, which minimizes the following RMS (root mean square) of error by changing both *K* and dRut.

$$RMS = \sqrt{\frac{1}{n}\sum_{i=1}^{n}\left[\left(Rut_{c,i} \times \frac{K}{1.4} \times \frac{1}{0.7} - dRut\right) - Rut_{m,i}\right]^2} \qquad \textbf{(11)}$$

where Rut_c and Rut_m are calculated and measured rut, respectively,
subscript i indicates the i^{th} value of measured rut,
K is the shift factor defined in Equation (4), and
dRut is the amount of initial rut removed by the 2000 NCAT research team.

As shown in Equation (11), a factor of 0.7 was assumed for the ratio between downward rut and the total rut. The reason that *K* can be applied directly to the total downward rut is that compression in the top AC layer accounts for most of that rut (see Section 6.6 for details).

Comparisons between final adjusted calculated ruts and measured ruts are shown in Figure 6.8 to Figure 6.11. Values for *K* and dRut along with final RMS are listed in Table 6.2. The values for dRut are generally small and are regarded as being reasonable. The values for K, however, seem to be quite different between sections with unmodified binder (N4 and N6) and those with modified binder (N8 and N9).

Table 6.2: Calibration Parameters Used to Match Measured Ruts

Section	K	dRut (mm)	RMS (mm)
N4	1.7	2.5	0.48
N6	1.3	1.8	0.48
N8	0.46	0.13	0.089
N9	0.32	0.25	0.088

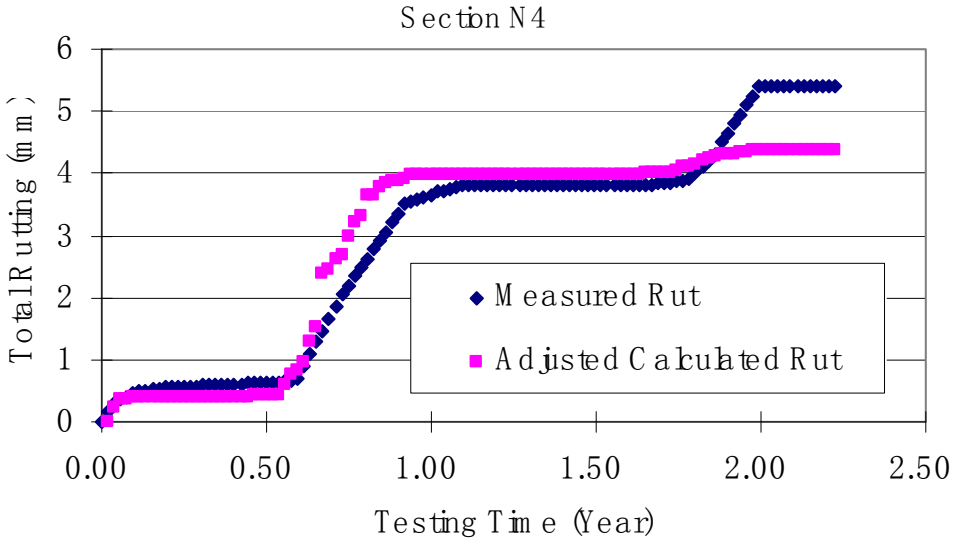

Figure 6.8: Comparison of adjusted calculated rut and measured rut for Section N4.

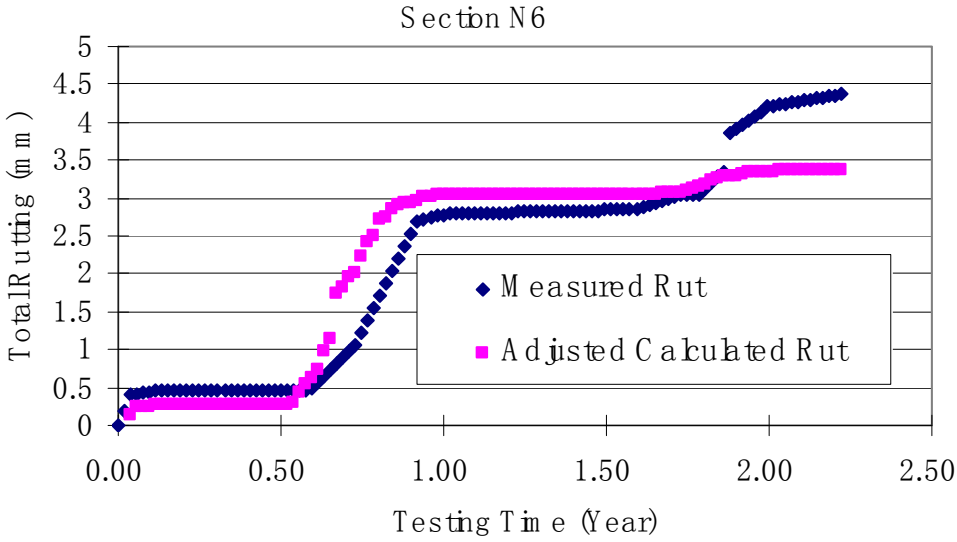

Figure 6.9: Comparison of adjusted calculated rut and measured rut for Section N6.

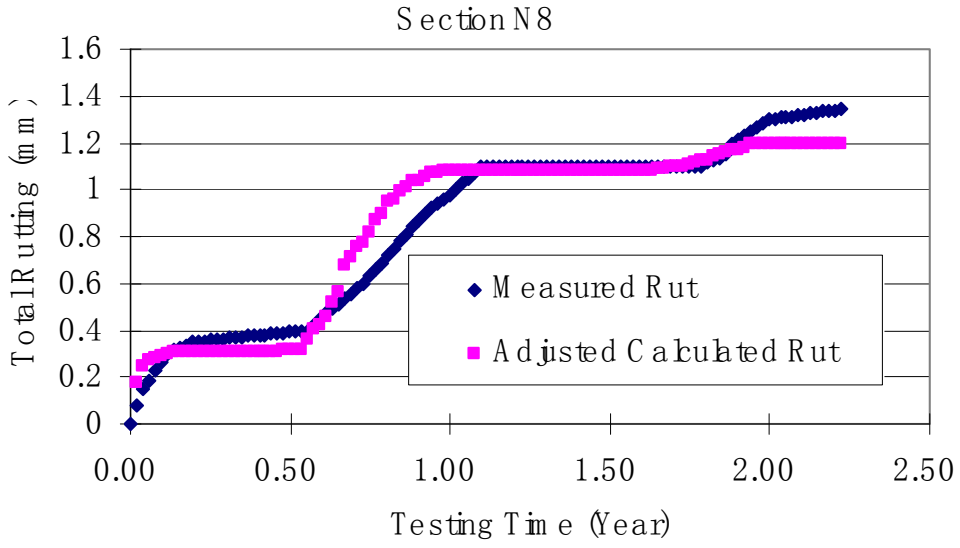

Figure 6.10: Comparison of adjusted calculated rut and measured rut for Section N8.

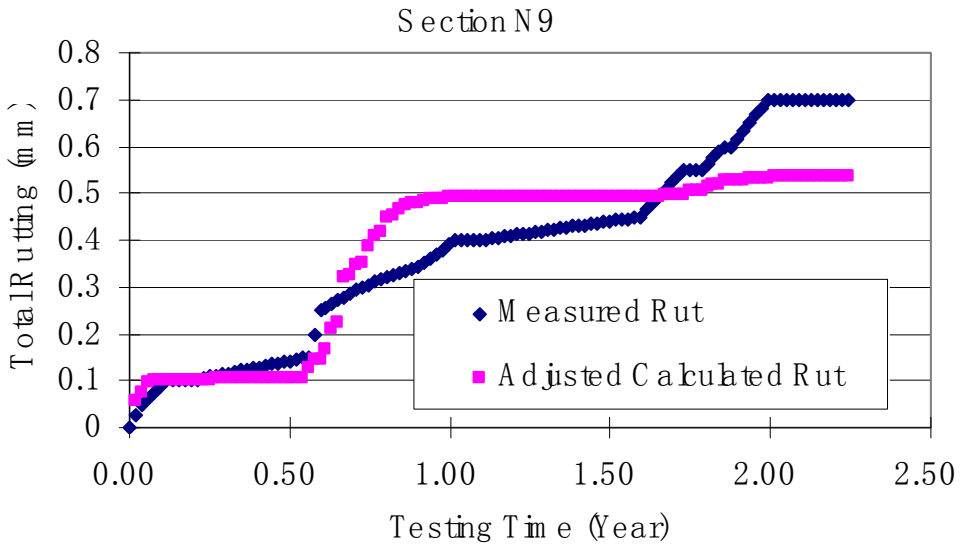

Figure 6.11: Comparison of adjusted calculated rut and measured rut for Section N9.

6.9 Validation Using *K* from Previous Projects

CalME has been calibrated and validated using data collected from several other sources, including WesTrack and HVS tests conducted by UCPRC. It would be helpful to know whether the same shift factor "K" used in previous projects can be used to predict rutting results in NCAT sections. It is preferable to use a single shift factor in routine design.

When calibrating *CalME* using WesTrack data, a different rutting model for AC was used to better match the measured performance. Specifically, a power function (i.e., type "t" in *CalME*) rather than a gamma function was used. In WesTrack calibration, *K* in Equation (4) and and *A* in Equation (6) were conbined into a single variable as *K*A*. A value of 0.9 was implicitly assumed for *K*. Due to the difference in rutting models, a *K* value of 0.9 will not be verified in this study.

When calibrating *CalME* using HVS test data (*1*), a gamma function was used for AC rutting and a shift factor of 1.4 was used. To check whether this factor can be used for the NCAT test sections selected in this study, the same optimization process as described in Section 6.8 is performed for each selected NCAT section. The only difference is that *K* is fixed at 1.4 here rather than being allowed to vary.

Comparisons between final adjusted calculated ruts and measured ruts are shown in Figure 6.12 to Figure 6.15. Values for *K* and dRut, along with final RMS, are listed in Table 6.3. The values for RMS are generally small and are regarded as being reasonable. The values for dRut are roughly the same among all sections. Based on these observations, it is believed that using a shift factor of 1.4 leads to satisfatory prediction of rutting performance in all the selected NCAT sections in this study.

Table 6.3: Calibration Parameters Used to Match Measured Ruts

Section	K	dRut (mm)	RMS (mm)
N4	1.4	1.7	0.55
N6	1.4	2.4	0.50
N8	1.4	2.6	0.23
N9	1.4	2.7	0.11

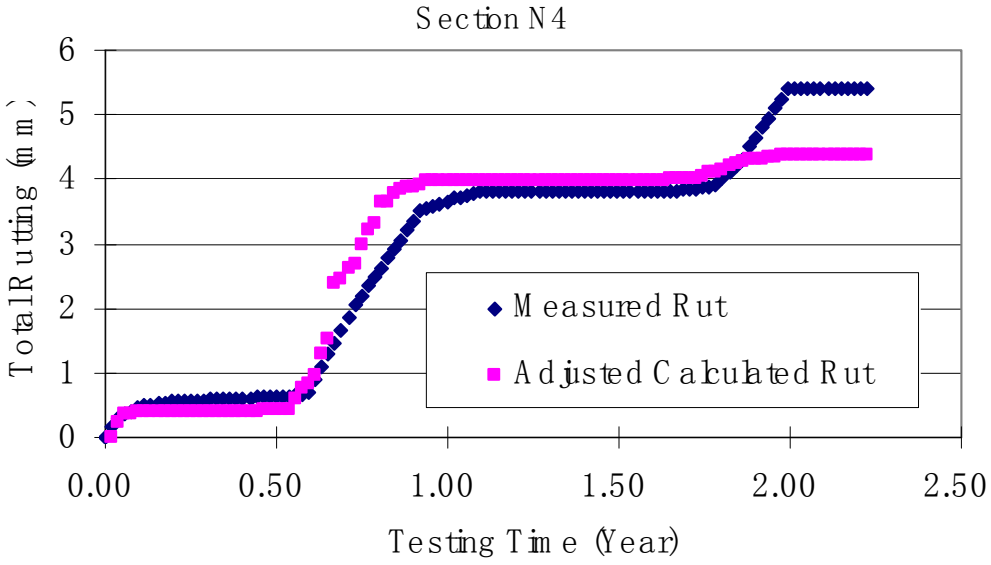

Figure 6.12: Comparison of adjusted calculated rut and measured rut for Section N4.

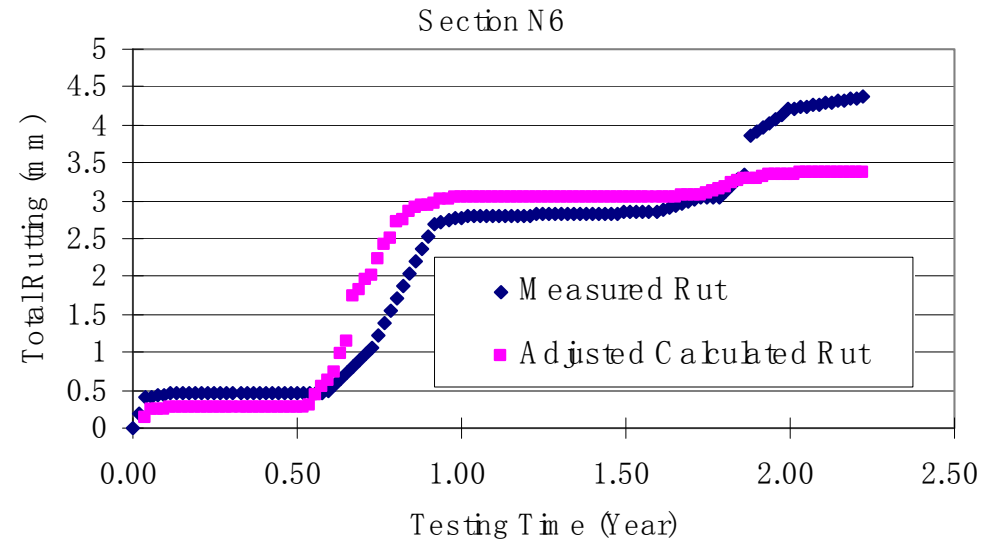

Figure 6.13: Comparison of adjusted calculated rut and measured rut for Section N6.

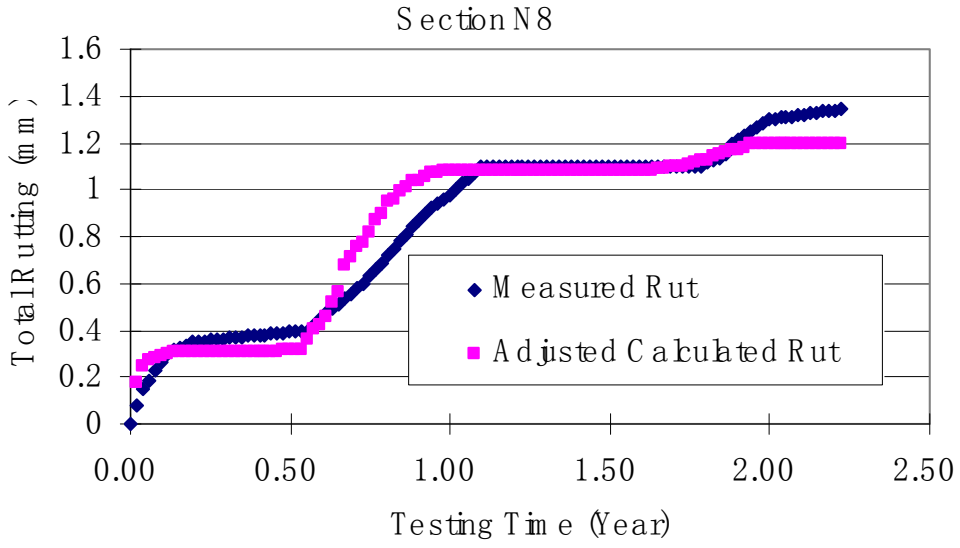

Figure 6.14: Comparison of adjusted calculated rut and measured rut for Section N8.

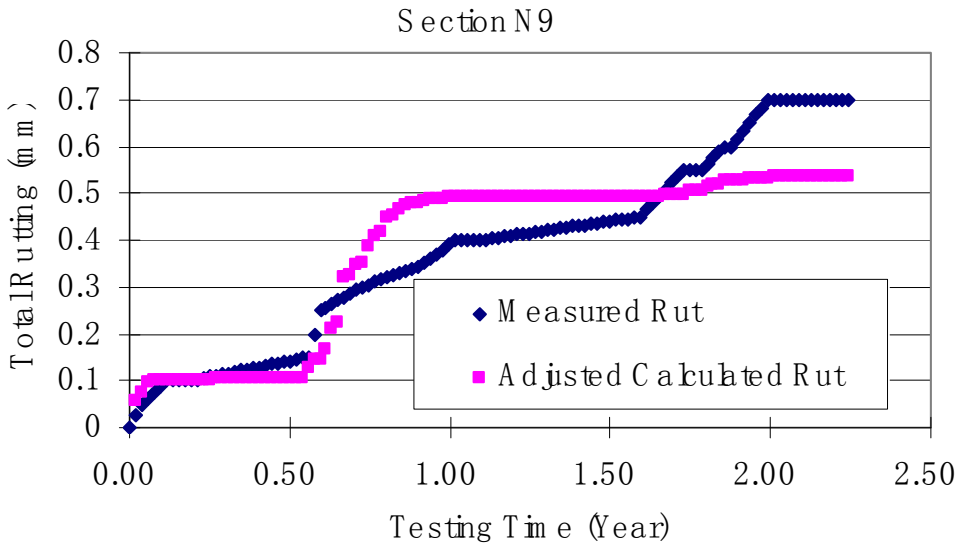

Figure 6.15: Comparison of adjusted calculated rut and measured rut for Section N9.

7 CONCLUSIONS AND RECOMMENDATIONS

This tech memo first validates the rutting models used in *CalME*. The general trend and the overall amount of calculated rut match the measured values very well. This implies that the rutting model for AC mixes is reasonable. However, the rutting models for aggregate base and subgrade cannot be validated using the selected data, since only about 5 percent of the total rut occurred in these two layers.

The model was calibrated by matching the calculated ruts with the measured results. The *K* values required ranged from 1.3 to 1.7 for sections with unmodified binder in the surface AC layer, and from 0.32 to 0.46 for sections with modified binder. Although the *K* values for sections with modified binders are quite different from the ones for unmodified binders, it is believed that more data are required to verify the necessity of using different *K* values based on whether the binder in an AC mix is modified or not. This conclusion is based on the fact that the total ruts in the selected NCAT sections with unmodified binders were very small (1.5 mm maximum).

The model was further verified by using shift factor *K* from calibration studies using HVS data. It was found that the same shift factor, i.e., $K = 1.4$, used in calibrating HVS test data led to a satisfactory match between predicted and measured rutting performance for the NCAT sections.

Because of the time constraints in this study, RSST-CH tests were conducted at one stress level only and did not provide sufficient information to determine the β parameter in the AC rutting model. A default value of 1.03 was used. It is recommended that RSST-CH tests be conducted at various stress levels in future studies. It is also recommended that study be made of what value should be used for β when only one stress level is used in RSST-CH tests. This can be done by fitting the AC rutting model through RSST-CH data for various types of AC mixes to learn how β varies with different mix properties, including binder type, gradation type, and so on.

Once the β value has been finalized through more RSST-CH test data, it is recommended that the linear relation between β and calculated rut shown in Figure 6.2 be used to adjust the *CalME* results and to verify the value for shift factor *K*.

REFERENCES

1. Ullidtz, P. et al., *Calibration of Incremental-Recursive Flexible Damage Models in CalME Using HVS Experiments.,* in report prepared for the California Department of Transportation (Caltrans) Division of Research and Innovation. 2006. University of California Pavement Research Center, Davis and Berkeley.
2. Powell, R. *Predicting Field Performance on the NCAT Pavement Test Track.* 2006. Auburn University.
3. Brown, E.R., et al. *NCAT Test Track Design, Construction, and Performance.* 2002. National Center for Asphalt Technology (NCAT), Auburn University.
4. Powell, B. As-Built Properties of Experimental Sections on the 2000 NCAT Pavement Test Track. 2001. National Center for Asphalt Technology, Auburn University, Alabama.
5. Division, A.I.E.C. *Guide for Mechanistic-Empirical Design of New and Rehabilitated Pavement Structures.* 2004. National Cooperative Highway Research Program, Transportation Research Board, National Research Council.
6. Deacon, J.A., et al., *Analytically based approach to rutting prediction.* Transportation Research Board, 2002. 1806.
7. Brown, E.R., et al. *NCAT Test Track Design, Construction, and Performance.* 2002. National Center for Asphalt Technology, Auburn University, Alabama.
8. Timm, D.H., and A.L. Priest. *Material Properties of the 2003 NCAT Test Track Structural Study.* 2006. National Center for Asphalt Technology (NCAT), Auburn University.
9. Harvey, J.T., et al. *CAL/APT Program: Test Results from Accelerated Pavement Test on Pavement Structure Containing Asphalt Treated Permeable Base (ATPB) Section 500RF.* 1997. Pavement Research Center, CAL/APT Program, Institute of Transportation Studies, University of California, Berkeley.
10. Tayebali, A., J.A. Deacon, and C.L. Monismith. *Development and evaluation of dynamic flexural beam fatigue test system.* Transportation Research Record, 1996 (1545): p. 89-97.
11. Epps, J.A., et al. *NCHRP Report 455: Recommended Performance-Related Specification for Hot-Mix Asphalt Construction: Results of the Westrack Project.* 2002. National Cooperative Highway Research Program.
12. Priest, A.L., D.H. Timm, and B.E. William. *Mechanistic Comparison of Wide-base Single vs. Standard Dual Tire Configurations.* 2005. National Center for Asphalt Technology (NCAT), Auburn University.
13. Timm, D.H. and A.L. Priest. *Wheel Wander at the NCAT Test Track.* 2005. National Center for Asphalt Technology (NCAT), Auburn University.
14. Ullidtz, P., et al. *Calibration of CalME Models Using WesTrack Performance Data.* 2007. California Department of Transportation Division of Research and Innovation Office of Roadway Research. p. 179.

APPENDIX A: SURFACE MIX CHARACTERISTICS

Section N4

Laboratory Diary

General Description of Mix and Materials

Design Method:	Superpave
Compactive Effort:	100 gyrations
Binder Performance Grade:	67-22
Modifier Type:	NA
Aggregate Type:	Lms/Slag
Gradation Type:	ARZ

Avg. Lab Properties of Plant Produced Mix

Sieve Size:	% Passing:
1"	100
3/4"	100
1/2"	99
3/8"	91
No. 4	68
No. 8	52
No. 16	35
No. 30	23
No. 50	15
No. 100	9
No. 200	6.0

Asphalt Binder Content:	6.8%
Compacted Pill Bulk Gravity:	2.296
Theoretical Maximum Gravity:	2.400
Computed Air Voids:	4.3%

Construction Diary

Relevant Conditions for Construction

Completion Date:	Thursday, May 18, 2000
24 Hour High Temperature (F):	85
24 Hour Low Temperature (F):	55
24 Hour Rainfall (in):	0.00
Lift Type:	dual
Design Thickness of Test Mix (in):	4.0

Plant Configuration and Placement Details

Component:		% Setting:
Liquid Binder Setting		7.1%
Slag	78	32.0%
Slag	8910	28.0%
Limestone	Manufactured Sand	40.0%

Approximate Length (ft):	199
Surveyed Thickness of Section (in):	4.2
Std Dev of Section Thickness (in):	0.1
Type of Tack Coat Utilized:	CQS-1h
Target Tack Application Rate:	0.03 gal/sy
Avg Mat Temperature Behind Paver (F):	288
Average Section Compaction:	93.4%

General Notes:

1) Mixes are listed chronologically in order of completion date (i.e., construction began with E2 and ended with E1).
2) Sections are referenced by quadrant and sequence number, where "E2" refers to section 2 of the east quadrant.
3) "dual" lift type indicates that the lower and upper lifts were constructed with the same experimental mix.
4) The total thickness of all experimental sections is 4 inches by design, with the exception of S8, S9, S10, S11.
5) ARZ, TRZ, and BRZ refer to gradations intended to pass above, through, and below the restricted zone.
6) SMA and OGFC refer to stone matrix asphalt and open-graded friction course, respectively.

Section N6

Laboratory Diary

General Description of Mix and Materials

Design Method:	Superpave
Compactive Effort:	100 gyrations
Binder Performance Grade:	67-22
Modifier Type:	NA
Aggregate Type:	Lms/Slag
Gradation Type:	BRZ

Avg. Lab Properties of Plant Produced Mix

Sieve Size:	% Passing:
1"	100
3/4"	100
1/2"	99
3/8"	85
No. 4	54
No. 8	37
No. 16	25
No. 30	17
No. 50	13
No. 100	10
No. 200	8.2

Asphalt Binder Content:	6.8%
Compacted Pill Bulk Gravity:	2.270
Theoretical Maximum Gravity:	2.348
Computed Air Voids:	3.3%

Construction Diary

Relevant Conditions for Construction

Completion Date:	Thursday, June 01, 2000
24 Hour High Temperature (F):	92
24 Hour Low Temperature (F):	67
24 Hour Rainfall (in):	0.00
Lift Type:	dual
Design Thickness of Test Mix (in):	4.0

Plant Configuration and Placement Details

Component:		% Setting:
Liquid Binder Setting		6.5%
Slag	78	53.0%
Slag	8910	17.0%
Limestone	Modified 8910	30.0%

Approximate Length (ft):	197
Surveyed Thickness of Section (in):	4.1
Std Dev of Section Thickness (in):	0.2
Type of Tack Coat Utilized:	CQS-1h
Target Tack Application Rate:	0.03 gal/sy
Avg Mat Temperature Behind Paver (F):	289
Average Section Compaction:	94.4%

General Notes:

1) Mixes are listed chronologically in order of completion date (i.e., construction began with E2 and ended with E1).
2) Sections are referenced by quadrant and sequence number, where "E2" refers to section 2 of the east quadrant.
3) "dual" lift type indicates that the lower and upper lifts were constructed with the same experimental mix.
4) The total thickness of all experimental sections is 4 inches by design, with the exception of S8, S9, S10, S11.
5) ARZ, TRZ, and BRZ refer to gradations intended to pass above, through, and below the restricted zone.
6) SMA and OGFC refer to stone matrix asphalt and open-graded friction course, respectively.

Section N8

Laboratory Diary

General Description of Mix and Materials

Design Method:	Superpave
Compactive Effort:	100 gyrations
Binder Performance Grade:	76-22
Modifier Type:	SBR
Aggregate Type:	Lms/Slag
Gradation Type:	BRZ

Avg. Lab Properties of Plant Produced Mix

Sieve Size:	% Passing:
1"	100
3/4"	100
1/2"	99
3/8"	85
No. 4	55
No. 8	37
No. 16	24
No. 30	17
No. 50	13
No. 100	10
No. 200	7.5

Asphalt Binder Content:	6.6%
Compacted Pill Bulk Gravity:	2.256
Theoretical Maximum Gravity:	2.351
Computed Air Voids:	4.0%

Construction Diary

Relevant Conditions for Construction

Completion Date:	Monday, June 05, 2000
24 Hour High Temperature (F):	77
24 Hour Low Temperature (F):	60
24 Hour Rainfall (in):	0.08
Lift Type:	dual
Design Thickness of Test Mix (in):	4.0

Plant Configuration and Placement Details

Component:		% Setting:
Liquid Binder Setting		6.4%
Slag	78	53.0%
Slag	8910	17.0%
Limestone	Modified 8910	30.0%

Approximate Length (ft):	203
Surveyed Thickness of Section (in):	3.9
Std Dev of Section Thickness (in):	0.2
Type of Tack Coat Utilized:	CQS-1h
Target Tack Application Rate:	0.03 gal/sy
Avg Mat Temperature Behind Paver (F):	319
Average Section Compaction:	94.7%

General Notes:

1) Mixes are listed chronologically in order of completion date (i.e., construction began with E2 and ended with E1).
2) Sections are referenced by quadrant and sequence number, where "E2" refers to section 2 of the east quadrant.
3) "dual" lift type indicates that the lower and upper lifts were constructed with the same experimental mix.
4) The total thickness of all experimental sections is 4 inches by design, with the exception of S8, S9, S10, S11.
5) ARZ, TRZ, and BRZ refer to gradations intended to pass above, through, and below the restricted zone.
6) SMA and OGFC refer to stone matrix asphalt and open-graded friction course, respectively.

Section N9

Laboratory Diary

General Description of Mix and Materials

Design Method:	Superpave
Compactive Effort:	100 gyrations
Binder Performance Grade:	76-22
Modifier Type:	SBS
Aggregate Type:	Lms/Slag
Gradation Type:	BRZ

Avg. Lab Properties of Plant Produced Mix

Sieve Size:	% Passing:
1"	100
3/4"	100
1/2"	99
3/8"	87
No. 4	57
No. 8	40
No. 16	26
No. 30	19
No. 50	14
No. 100	11
No. 200	8.8

Asphalt Binder Content:	6.7%
Compacted Pill Bulk Gravity:	2.279
Theoretical Maximum Gravity:	2.354
Computed Air Voids:	3.2%

Construction Diary

Relevant Conditions for Construction

Completion Date:	Wednesday, June 07, 2000
24 Hour High Temperature (F):	84
24 Hour Low Temperature (F):	60
24 Hour Rainfall (in):	0.00
Lift Type:	dual
Design Thickness of Test Mix (in):	4.0

Plant Configuration and Placement Details

Component:		% Setting:
Liquid Binder Setting		6.4%
Slag	78	53.0%
Slag	8910	17.0%
Limestone	Modified 8910	30.0%

Approximate Length (ft):	197
Surveyed Thickness of Section (in):	3.9
Std Dev of Section Thickness (in):	0.2
Type of Tack Coat Utilized:	CQS-1h
Target Tack Application Rate:	0.03 gal/sy
Avg Mat Temperature Behind Paver (F):	314
Average Section Compaction:	94.5%

General Notes:

1) Mixes are listed chronologically in order of completion date (i.e., construction began with E2 and ended with E1).
2) Sections are referenced by quadrant and sequence number, where "E2" refers to section 2 of the east quadrant.
3) "dual" lift type indicates that the lower and upper lifts were constructed with the same experimental mix.
4) The total thickness of all experimental sections is 4 inches by design, with the exception of S8, S9, S10, S11.
5) ARZ, TRZ, and BRZ refer to gradations intended to pass above, through, and below the restricted zone.
6) SMA and OGFC refer to stone matrix asphalt and open-graded friction course, respectively.

APPENDIX B: A SIMPLE MODEL FOR PAVEMENT DAMAGE, BY PER ULLIDTZ, DYNATEST INTERNATIONAL

Per Ullidtz
Naverland 32
DK 2600 Glostrup, Denmark
Tel: +45 7025 3355
Fax: +45 7025 3356
e-mail: pullidtz@dynatest.com

Paper No. 05-0084, AFD80

Abstract

A simple, phenomenological damage model, based on number of load applications, critical response and material modulus, is used on three sets of experimental data:

1. the decrease in modulus of an asphalt concrete under laboratory, direct tension fatigue testing,
2. the decrease in modulus of a Pozzolan-lime stabilized sand under accelerated loading in a full scale pavement testing facility, and
3. the increase in permanent strain at three different levels of two subgrade materials, also under full scale accelerated loading.

The model is shown to be capable of describing the damage reasonably well for all three cases, although with some limitations. For the direct tension tests on AC, the rate of damage was underpredicted for two samples under controlled stress testing (out of six), whereas the prediction for all ten controlled strain tests was very good. For freeze/thaw conditions the model for permanent strain in the subgrade also tended to underpredict the damage rate.

The simple damage model may be useful for incremental-recursive pavement design or for Pavement Management Systems.

Introduction

Pavement deterioration is a very complex process. It is a function of the materials, layer thicknesses, number of loads (and their configuration, size, contact stress, lateral distribution, frequency), as well as of environmental effects and ageing. The deterioration is also a gradual process where the deterioration itself may change the materials and influence the loading.

To model this deterioration is equally complex and may require extensive and time-consuming computer simulation. Simplified, phenomenological models may, therefore, be useful for example in connection with Pavement Management Systems, where thousands of pavement sections must be simulated over long periods (20-40 years) with numerous maintenance or rehabilitation alternatives.

This paper proposes a simple damage model:

$$Damage = A \times MN^{\alpha} \times \left(\frac{resp}{resp_{ref}} \right)^{\beta} \times \left(\frac{E}{E_i} \right)^{\gamma},$$

$MN \text{ is million load applications}$

$resp \text{ is response}$

$resp_{ref} \text{ is reference response}$

$E \text{ is modulus}$

$E_i \text{ is initial modulus}$

$A, \alpha, \beta, \text{and } \gamma \text{ are constants}$

Equation 1

"Damage" may be defined as decrease in the modulus of a material (normally a bitumen or cement bound material) or as increase in permanent (or plastic) deformation, which again may be related to rutting or roughness. The response may be normal stress or strain, tensile or compressive.

If both response, *resp,* and modulus, *E,* remain constant Equation 1 may be used as it is to predict damage as a function of the number of loads. When the response and/or the modulus change, for example as a function of load level, environmental condition (e.g. temperature or moisture changes), ageing or gradual deterioration, the model must be used incrementally, with the "time hardening" procedure (Monismith et al. 1975). For a new increment, the number of loads (in millions), MNo, required to reach the present level of damage, is first calculated, using the present level of response and modulus, during the increment. The damage at the end of the increment is then calculated for MNo + dMN loads, where dMN is the number of loads (in millions) during the increment. The new damage level is input, recursively, to the next increment.

The paper presents three cases where the damage model has been fitted to experimental data.

Decrease of Asphalt Concrete Modulus

A model was developed for an asphalt mixture, based on experiments reported by Richard Nilsson (2003).

The asphalt was a dense graded base course mixture (Swedish standard AG16) with a maximum grain size of 16 mm. A 160/220 pen bitumen was used with a binder content of 4.8% by weight of mixture. The mixture was manufactured in a batch plant and slabs were compacted using a rolling wheel. 75 mm diameter samples were cored horizontally from the slabs, and cut to a length of 150 mm, to avoid any end effects.

The samples were tested in uniaxial loading, using a UTM-25, after a few days of sample preparation and storage. The tests used here were all done with sinusoidal loading, either as constant strain tests or constant stress tests.

A total of 16 sinusoidal tests were carried out on this material. Their designation, temperature, frequency of loading and recorded void content are given in Table 1.

Designation	Temperature °C	Frequency Hz	Void content %	Mean stress or strain
A31	10	10	3.4	446 micron/m
A32	10	10	3.6	457 micron/m
A42	10	10	4.8	346 micron/m
B32	10	10	3.2	450 micron/m
B51	10	10	3.7	339 micron/m
B52	10	10	3.6	2200 kPa
C12	10	10	4.1	2200 kPa
C42	10	10	4.3	3000 kPa
D12	0	1	4.3	3000 kPa
D21	0	10	4.2	348 micron/m
D32	0	1	3.9	716 micron/m
E22	0	1	4.7	707 micron/m
E42	0	10	4.0	3400 kPa
F22	0	10	4.6	3000 kPa
F31	0	10	3.7	356 micron/m
F52	0	1	2.7	811 micron/m

Table 1

Damage was defined as the relative decrease in modulus, i.e. $(E_i - E)/E_i$.

The results of the 16 tests were entered in an Excel spreadsheet and the model parameters were determined using “Solver”, by minimizing the Root Mean Square (RMS) difference between the measured damage and the damage predicted by the model.

The resulting model parameters are given below:

$$\frac{E_i - E}{E_i} = \left(\frac{E_i}{3000\,MPa}\right)^{-0.2666} \times MN^{0.3103} \times \left(\frac{micro\varepsilon}{197.8\,micron/m}\right)^{1.451} \times \left(\frac{E}{E_i}\right)^{0.08684}$$

Equation 2

The RMS difference between measured and calculated damage was 0.041, or 4.1%.

All of the test results and the model data are shown in the following 16 plots. The abscissa is the number of loads and the ordinate is the modulus in MPa. The measured data is indicated by (open) squares and the model data by filled diamonds. The heading indicates the constant stress (kPa) or strain (microstrain, micron/m).

For most of the experiments Equation 2 describes the decrease in modulus very well, for controlled strain tests as well as for controlled stress tests. For two of the controlled stress tests, however, there is a marked difference between the model and the experiment. These are the tests E42 and F22, both at 0°C and 10 Hz.

As an alternative the ratio of the powers on strain and modulus was forced to be 0.5. This corresponds to the damage being proportional to the energy density (½×ε×σ = ½×ε^2×E).

$$\frac{E_i - E}{E_i} = \left(\frac{E_i}{3000\,MPa}\right)^{-0.4406} \times MN^{0.4016} \times \left(\frac{micro\varepsilon}{127.4\,microstrain}\right)^{1.7696} \times \left(\frac{E}{E_i}\right)^{0.8848}$$

Equation 3

This equation results in an RMS difference from the measured damage of 0.050, where Equation 2 results in 0.041. In both cases the difference is mostly due to the same two, controlled stress, tests.

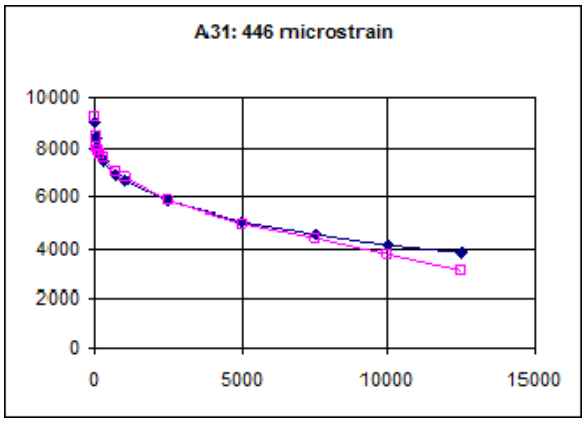
A31: 446 microstrain
10000
8000
6000
4000
2000
0
0
5000
10000
15000

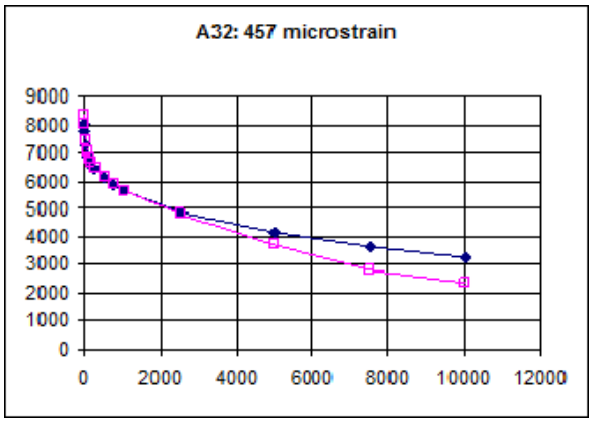
A32: 457 microstrain
9000
8000
7000
6000
5000
4000
3000
2000
1000
0
0
2000
4000
6000
8000
10000
12000

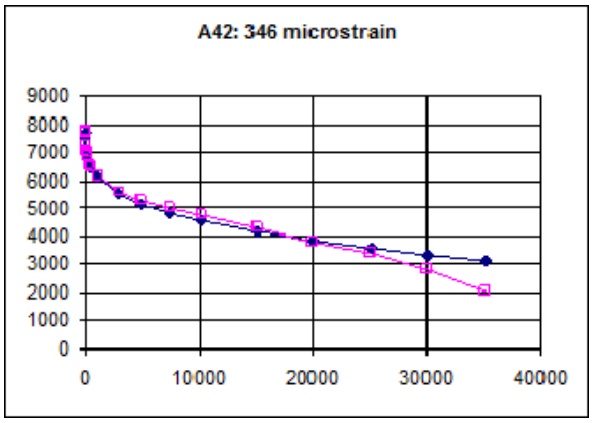
A42: 346 microstrain
9000
8000
7000
6000
5000
4000
3000
2000
1000
0
0
10000
20000
30000
40000

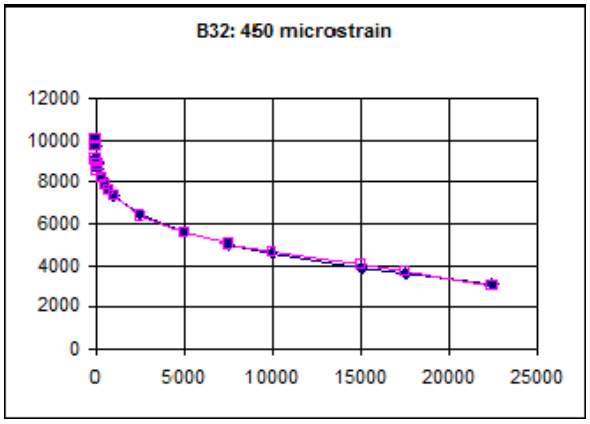
B32: 450 microstrain
12000
10000
8000
6000
4000
2000
0
0
5000
10000
15000
20000
25000

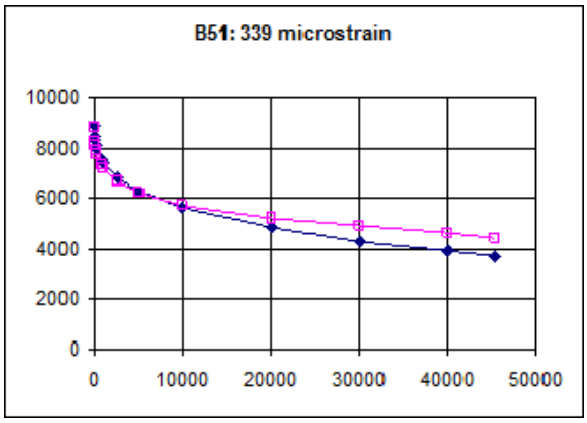
B51: 339 microstrain
10000
8000
6000
4000
2000
0
0
10000
20000
30000
40000
50000

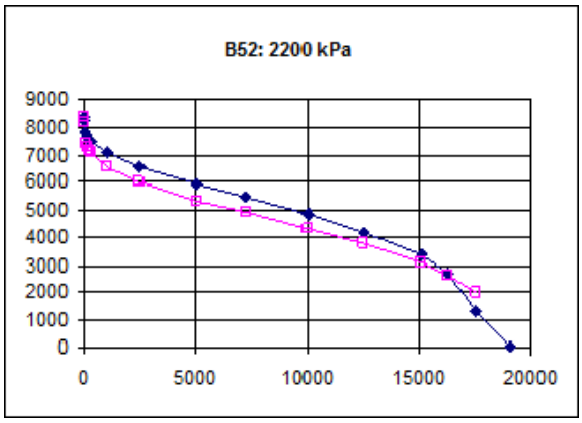
B52: 2200 kPa
9000
8000
7000
6000
5000
4000
3000
2000
1000
0
0
5000
10000
15000
20000

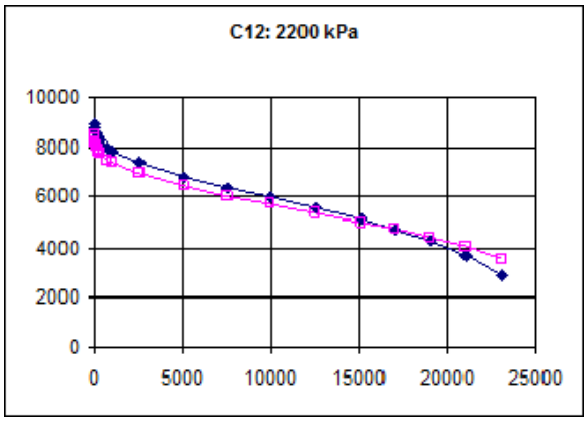
C12: 2200 kPa
10000
8000
6000
4000
2000
0
0
5000
10000
15000
20000
25000

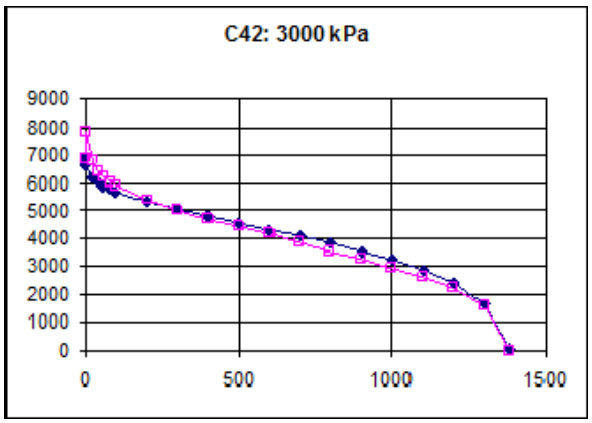
C42: 3000 kPa
9000
8000
7000
6000
5000
4000
3000
2000
1000
0
0
500
1000
1500

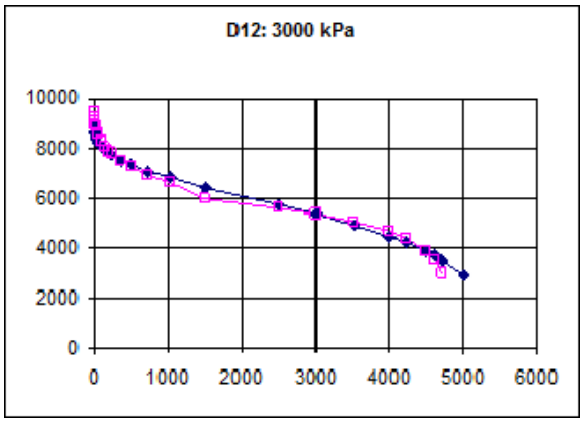
D12: 3000 kPa
10000
8000
6000
4000
2000
0
0
1000
2000
3000
4000
5000
6000

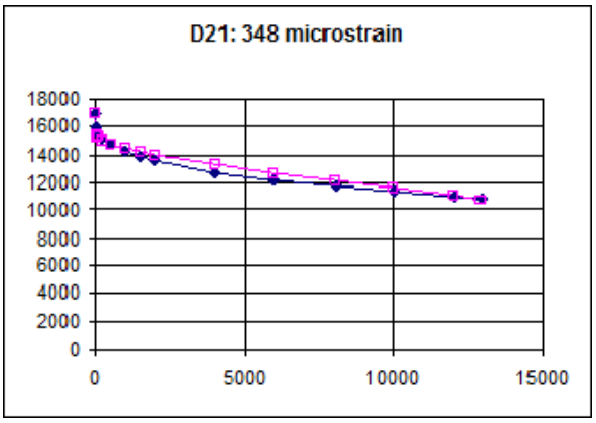
D21: 348 microstrain
18000
16000
14000
12000
10000
8000
6000
4000
2000
0
0
5000
10000
15000

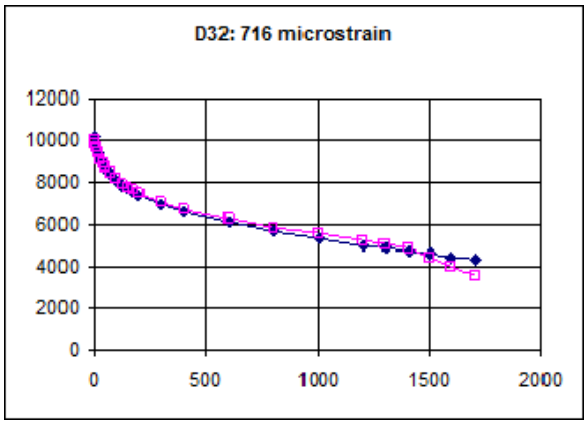
D32: 716 microstrain
12000
10000
8000
6000
4000
2000
0
0
500
1000
1500
2000

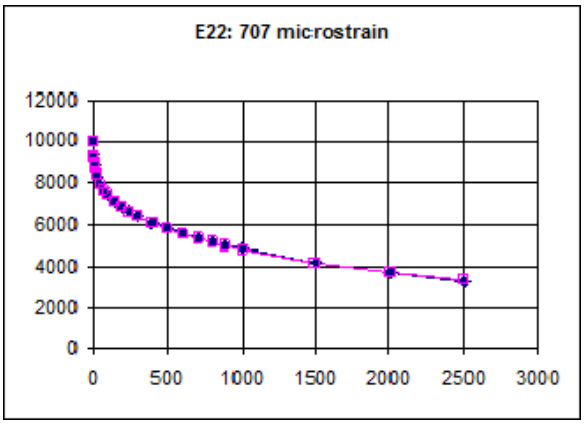
E22: 707 microstrain
12000
10000
8000
6000
4000
2000
0
0
500
1000
1500
2000
2500
3000

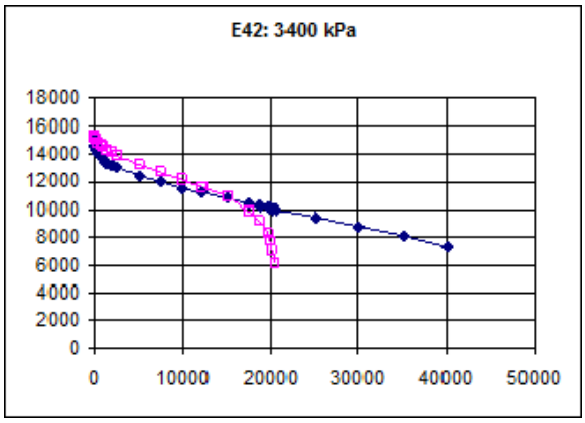
E42: 3400 kPa
18000
16000
14000
12000
10000
8000
6000
4000
2000
0
0
10000
20000
30000
40000
50000

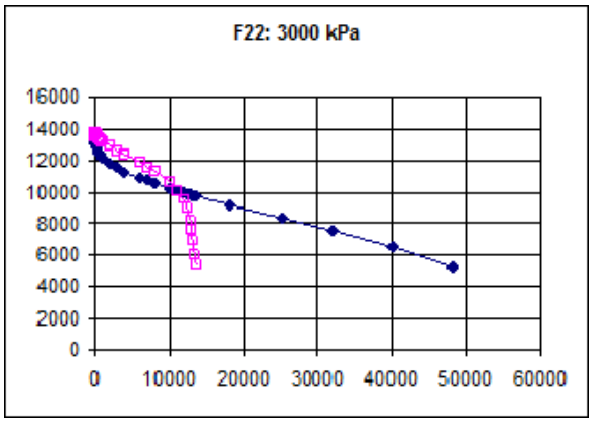
F22: 3000 kPa
16000
14000
12000
10000
8000
6000
4000
2000
0
0
10000
20000
30000
40000
50000
60000

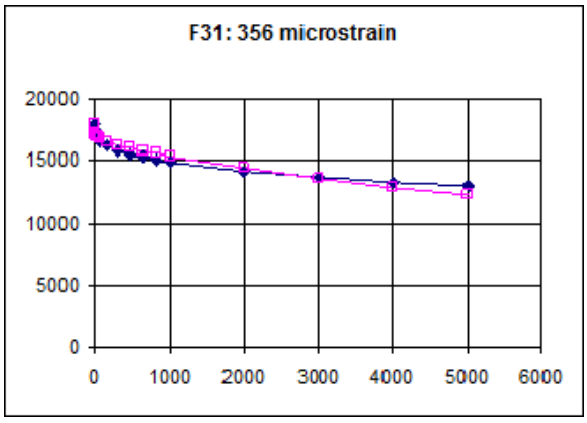
F31: 356 microstrain
20000
15000
10000
5000
0
0
1000
2000
3000
4000
5000
6000

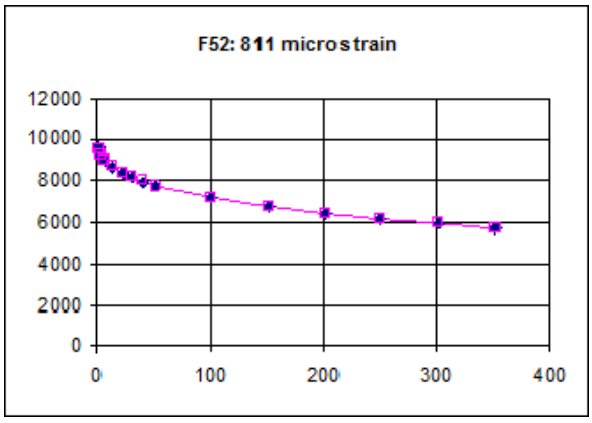
F52: 811 microstrain
12000
10000
8000
6000
4000
2000
0
0
100
200
300
400

The Asphalt Institute (TAI) criterion for permissible strain in laboratory controlled strain fatigue tests on asphalt concrete may be written as (Shook et al., 1982):

$$\mu\varepsilon_{permissible} = 98.2 micron/m \times C' \times MN^{-.304} \times \left(\frac{E}{3000\,MPa}\right)^{-0.259}$$

$$C' = 10^{\left(1.47 \times \left(\frac{Vb}{Vb+Vv} - 0.69\right)\right)}$$

Equation 4

where Vb is the volume percent of bitumen, and
Vv is the volume of voids.

This "classical" criterion has been used over many years for Mechanistic-Empirical design of flexible pavements, with a shift factor for in situ conditions. It is, therefore, interesting to compare this criterion to the simple damage model.

Assuming that "failure" is defined as a decrease in modulus to half the initial value, i.e. a damage of 0.5, Equation 2 and Equation 4 may be compared.

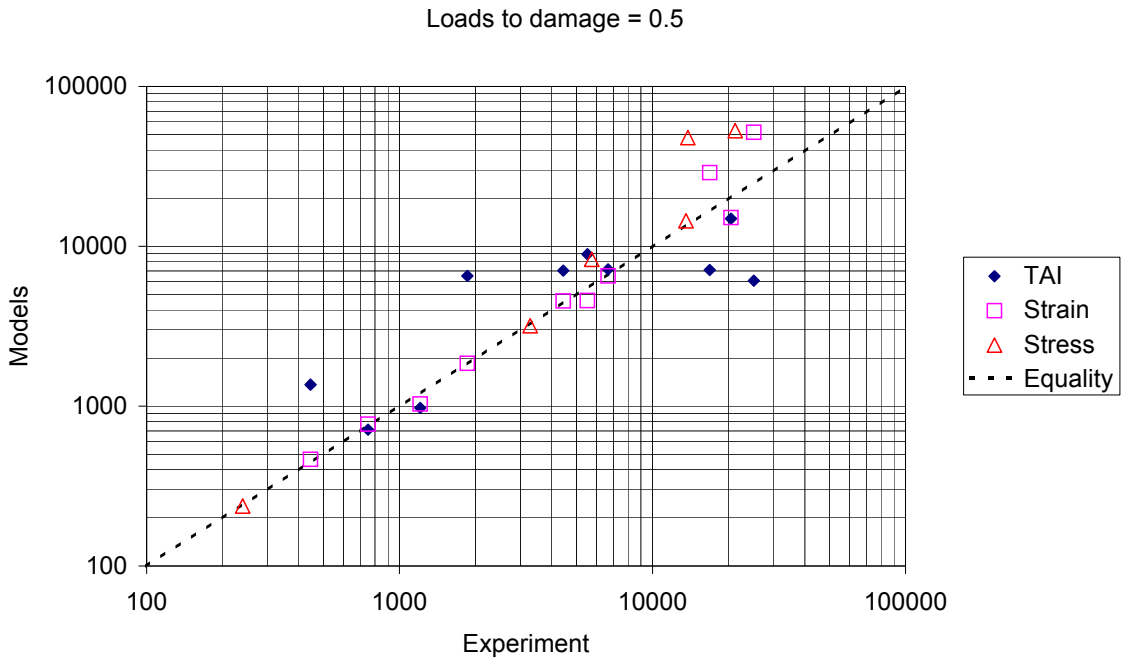

Figure 1. Experiments compared to model prediction and to The Asphalt Institute criterion (TAI).

Two of the controlled strain tests are seen to deviate from experimental data (in addition to the two controlled stress tests mentioned previously). These are the tests D21 and F31 where a damage of 0.5 was not reached and the number of loads to failure, therefore, had to be extrapolated.

The predictions made with The Asphalt Institute criterion is seen to be in reasonably good agreement with the experimental data and with the simple model.

Decrease of Pozzolan Treated Sand Modulus

The Danish International Development Agency (Danida) sponsored an experiment in the Danish Road Testing Machine (RTM), to develop a damage model for a sand material stabilized with pozzolan (6.5%) and lime (1.5%). Reactions between pozzolan and lime are similar to the reactions of Portland cement. These effects were known by the Romans, who used volcanic ash from Pozzuoli, mixed with lime, for many of their structures (e.g. the Pantheon which is still in pretty good condition after 2000 years). In the present experiment the volcanic ash was from Kilimanjaro in Tanzania.

The test pavement consisted of 25 mm of Asphalt Concrete on 150-190 mm of pozzolan stabilized sand on a silty clay subgrade (loam). Strain gauges were installed at the bottom of the stabilized sand layer, 6 longitudinal and 6 transverse, all installed in the wheel paths of the dual wheel.

The first 40,000 passages were at a wheel load of 20 kN, the next 40,000 at 40 kN and the remaining loads at 60 kN. The corresponding tire pressures were 500 kPa, 600 kPa and 800 kPa. At frequent intervals the strains at the bottom of the stabilized layer were measured, the pavement surface was inspected, FWD tests were carried out and the pavement surface profile was measured. Layer moduli were backcalculated using the program Elmod (Ullidtz & Stubstad, 1985), assuming a constant modulus of 1000 MPa for the AC layer (20-25°C).

The measured permanent deformation, in the weakest half of the test section, is shown as a function of the number of load passages in Figure 2. After 80,000 loads, just before the load level was increased to 60 kN, the permanent deformation was approximately 7 mm. The visual inspection showed the pavement to be in a very good condition with no cracking at the pavement surface.

At 92,000 load applications the first crack occurred at the pavement surface, and then, cracking and rutting developed very fast. At 96,000 load applications the experiment had to be stopped due to excessive surface deformation. When the experiment was stopped the pavement also had extensive cracking.

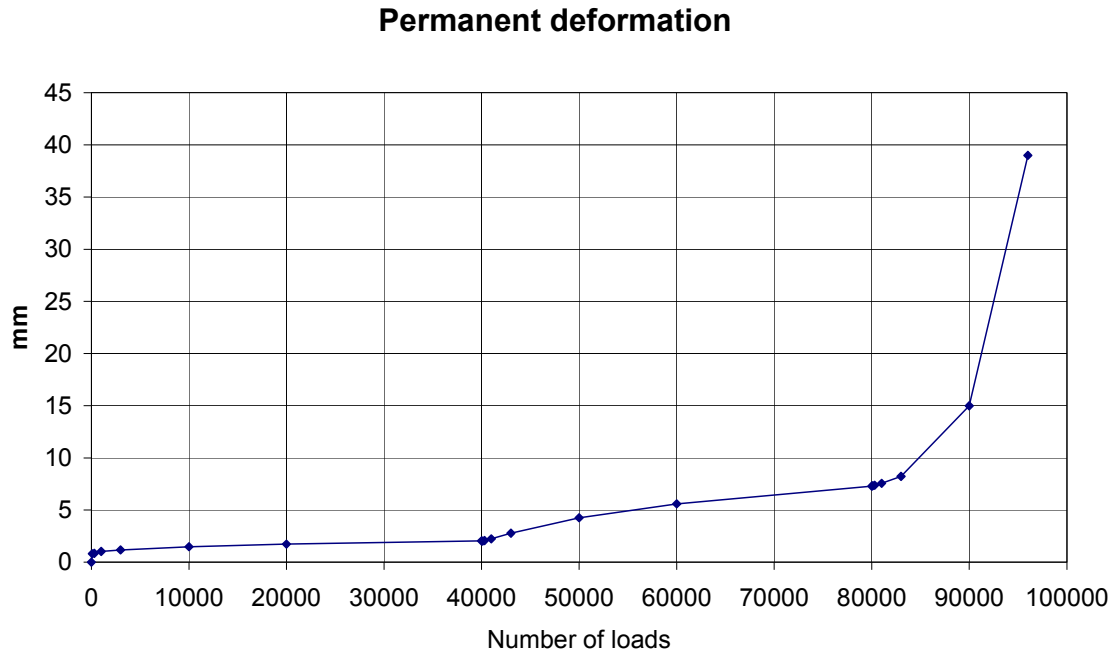

Figure 2. Permanent surface deformation.

The backcalculated moduli of the stabilized sand revealed, however, that a considerable amount of structural deterioration had taken place. At 80,000 load applications, where the visual condition was still good, the modulus had decreased to about 25% of the initial value.

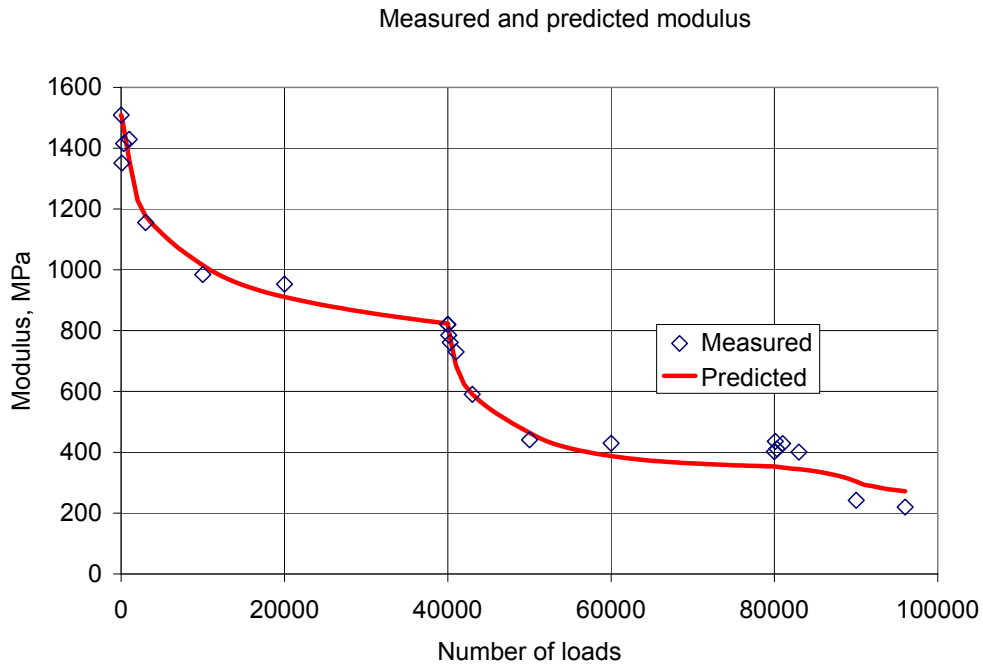

Figure 3. Modulus of pozzolan stabilized sand as a function of loads.

The following model parameters were used to predict the decrease in modulus:

$$\frac{E_i - E}{E_i} = MN \times \left(\frac{micro\varepsilon}{77\,micron/m} \right)^{5.6} \times \left(\frac{E}{E_i} \right)^{10}$$

Equation 5

As only one material was tested it was not possible to evaluate the influence of the initial modulus on the parameter A, or microε_{ref}, in the model.

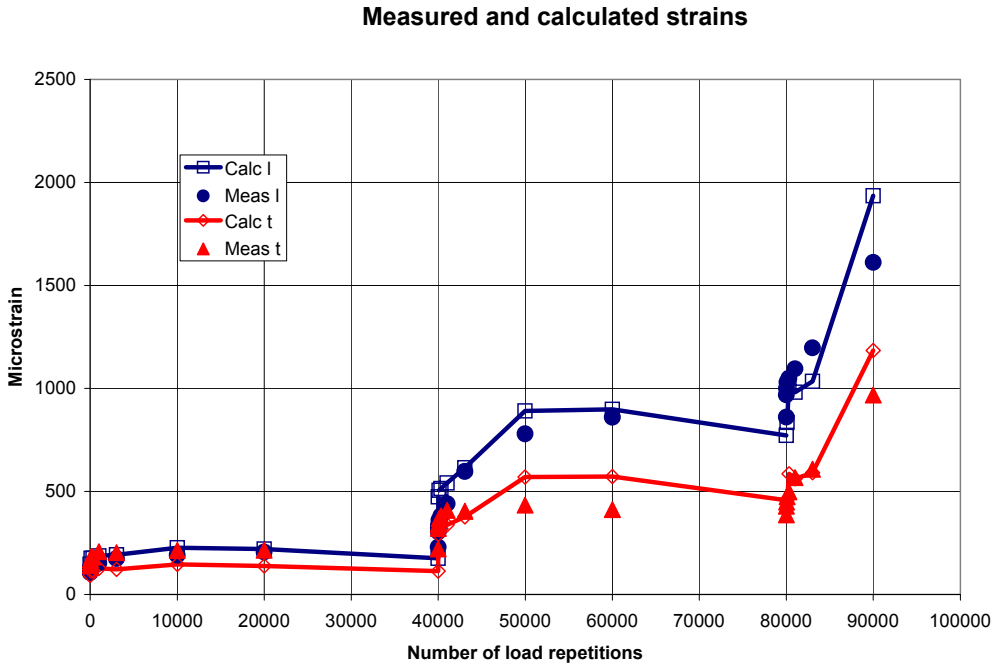

Figure 4. Comparison of measured and calculated strains.

Figure 4 shows a comparison of the measured horizontal, tensile strains at the bottom of the stabilized layer (Meas l for longitudinal and t for transverse) and the strains calculated using the layer moduli calculated from Equation 5 (Calc). The agreement is seen to be reasonably good. It should be noted that due to variability in layer thickness and moduli and due to formation of cracks, the scatter of the measured strains was large. The values shown are the average values.

In predicting the decrease in modulus of the stabilized layer, the maximum calculated strain was used. The maximum strain was approximately 10% larger than the longitudinal strain measured in the centre line of one of the wheels in the dual wheel.

The “French Design Manual for Pavement Structures”, 1997 has design criteria for fatigue damage of pozzolan stabilized sand. For a material like the one used in this experiment the criterion may be written approximately like:

$$micro\varepsilon_{permissible} = 57.5\, micron/m,\ for\ 1\ million\ load\ applications\ (MN = 1)$$

Equation 6

With Equation 5 this would correspond to a damage of 0.082, or 8.2%, which is probably a reasonable design level for this type of material.

Permanent Deformation of Subgrade

For the International Pavement Subgrade Study, a test pavement (RTM1) was constructed in 1994 in the Danish Road Testing Machine (RTM). This experiment was supplemented with a second, almost identical, test pavement (RTM2) constructed in 1997. After RTM2 had been subjected to 160,000 load repetitions and two freeze/thaw experiments causing a rut depth of 20 mm, the pavement was rehabilitated. An open-graded asphalt concrete layer, about 35 mm thick, was overlaid on the RTM2 deformed surface. The rehabilitated test pavement was called RTM3 (Zhang & Ullidtz, 2002).

The focus of these tests was on the subgrade, which in all experiments consisted of a Danish "Moraine Clay" classified as a clayey silty sand (AASHTO classification A-4(0)). It had an optimum moisture content of 9% and a maximum dry density of 2045 kg/m^3. It was constructed in nine layers of approx. 150 mm thickness each. The top three layers were instrumented with pressure cells and strain cells. The strain cells were capable of recording resilient as well as permanent strain.

Subgrade layer No.	Moisture content %	Degree of compaction %	Approximate CBR
1	11	97	5
2	10	97	9
3	9	91	15

Table 2. Subgrade of RTM2 and RTM3

The CBR values are estimated from laboratory tests at different moisture contents.

A very thin pavement was constructed on top of the subgrade, consisting of a 140 – 170 mm thick granular base course and an 84 mm thick asphalt concrete layer (for RTM2). The base course was a 0-32 mm crushed natural gravel and the AC had a maximum grain size of 16 mm and a 60 pen bitumen. The intention was to provoke permanent deformation in the subgrade.

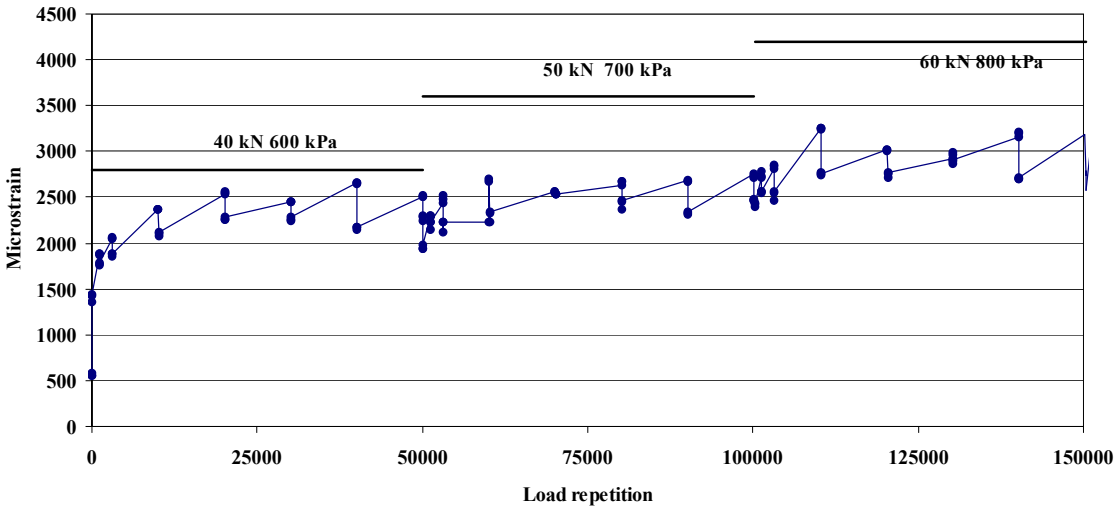

Figure 5. Resilient vertical strain in subgrade layer 1 during RTM2.

The vertical drops in the strains shown in Figure 5 are caused by rest periods, used for visual inspection, FWD tests and measurement of surface profile. The measured permanent vertical strain in each of the three top layers of the subgrade (shown for the top subgrade layer in Figure 6 and Figure 7), for all of the three experiments and all load levels were used for determining the parameters in the damage model, as a function of the measured resilient strain and the measured stress.

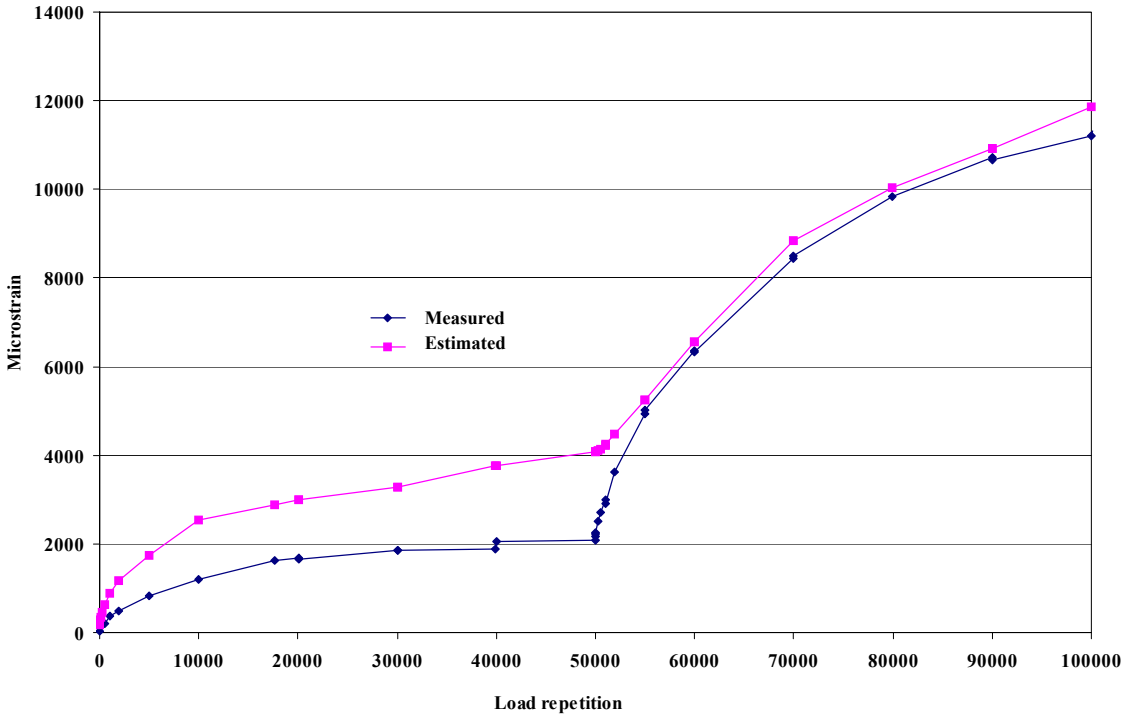

Figure 6. Permanent strain in subgrade layer 1 of RTM1.

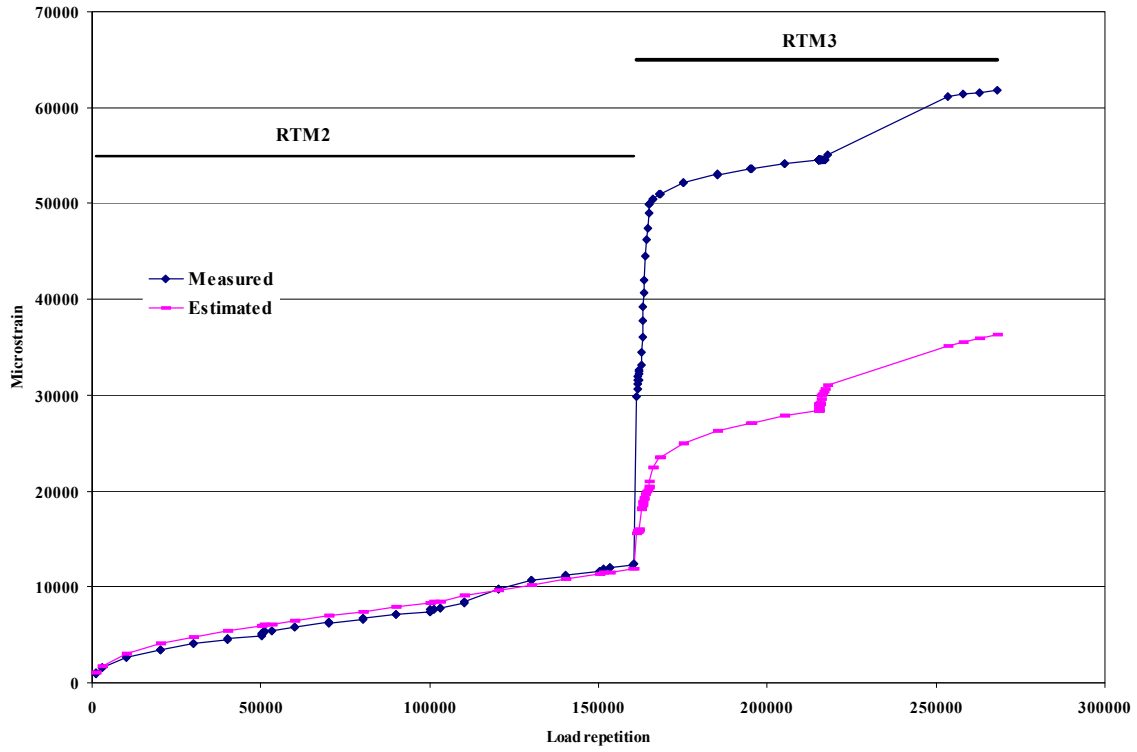

Figure 7. Permanent strain in subgrade layer 1 of RTM2 and RTM3.

The model parameters are given below:

$$micro\varepsilon_p = 6383\,micron/m \times MN^{0.333} \times \left(\frac{micro\varepsilon}{1000\,micron/m}\right)^{1.333} \times \left(\frac{E}{40MPa}\right)^{0.333}$$

Equation 7

microε_p is the permanent vertical strain (in micron/m or microstrain) and microε is the resilient vertical strain.

After 160,000 load applications in the RTM2 experiment the pavement was frozen to a depth comprising the top three subgrade layers. A frost heave of 5-15 mm was recorded at the surface, and all of the vertical strain cells reverted from a positive (compressive) strain to negative (tensile) strains of –10,000 to –20,000 microstrain (see Figure 8). During thawing 60 kN loads were applied at a rate of approximately 20 loads per day (though 150 loads the first day) to a total of 1800 load applications. The pavement was then frozen for a second time, with a frost heave of 5-25 mm, and loaded with 15 load applications per day the first 20 days, then at 150 loads/day and later 300 loads/day. In RTM3 a freeze/thaw experiment was carried out at 215,000 load applications.

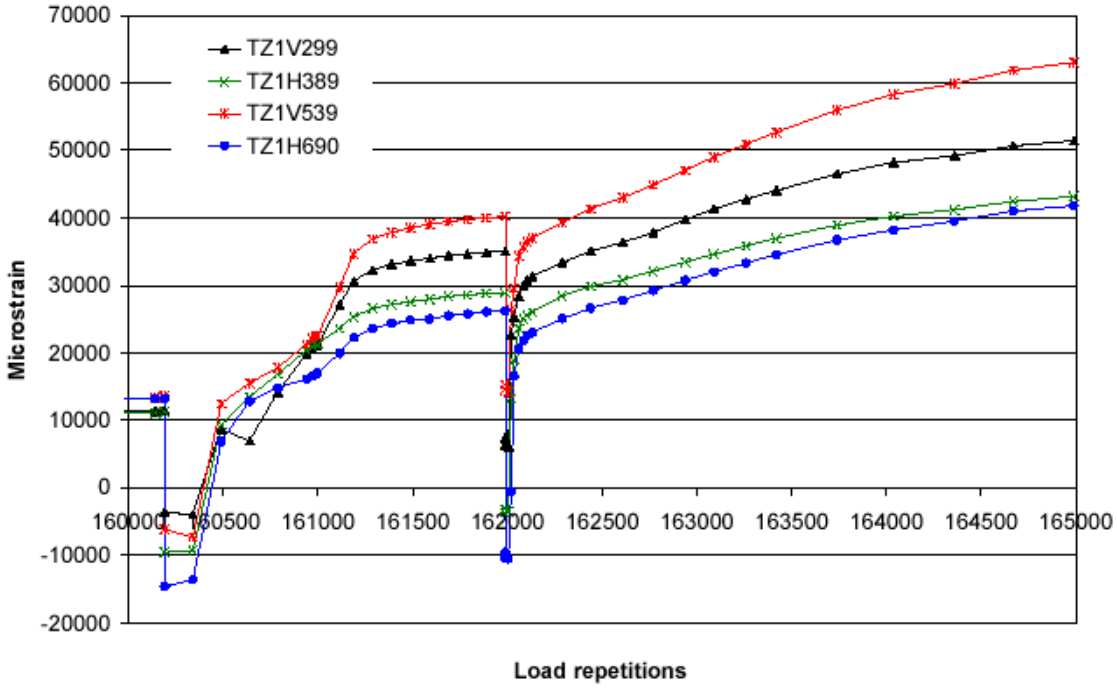

Figure 8. Permanent strain in subgrade layer 1 under two first freeze/thaw cycles.

It is quite evident from Figure 7 that the model is not capable of describing the permanent deformation caused during thawing, even though the number of load applications (in the model) were reset to zero after each frost period (because of the heave). The permanent strain resulting from the two first frost periods is underestimated by more than 20,000 microstrain. The prediction is better during the third freeze/thaw, in RTM3.

The ratio of stress over permanent strain, or the "plastic modulus", may be expressed as a nonlinear relationship of the vertical stress. The deformation may be determined by integrating the strains and for the nonlinear relationship a closed form solution exists (Ullidtz, 1998). Using this, the following model parameters may be determined:

$$d_p = 1.1mm \times MN^{0.333} \times \left(\frac{micro\varepsilon}{1000\,micron/m} \right)^{1.333} \times \left(\frac{E}{40MPa} \right)^{0.333}$$

Equation 8

where d_p is the permanent deformation at the top of the subgrade. It would be interesting if a larger, more detailed data set could be used to develop similar models for other pavement layers.

Model parameters were also determined for the rut depth (RD), measured under a 4 foot straight edge, and for the increase in International Roughness Index (ΔIRI), as a function of the resilient strain at the top of the subgrade and the subgrade modulus. These models are less reliable because deformation in the asphalt and the granular base layers contribute to RD and ΔIRI and these

contributions should, preferably, be treated separately. Unfortunately the available data did not allow that. The model parameters are given below:

$$RD = 4.1mm \times MN^{0.333} \times \left(\frac{micro\varepsilon}{1000\,micron/m} \right)^{1.333} \times \left(\frac{E}{40MPa} \right)^{0.333}$$

Equation 9

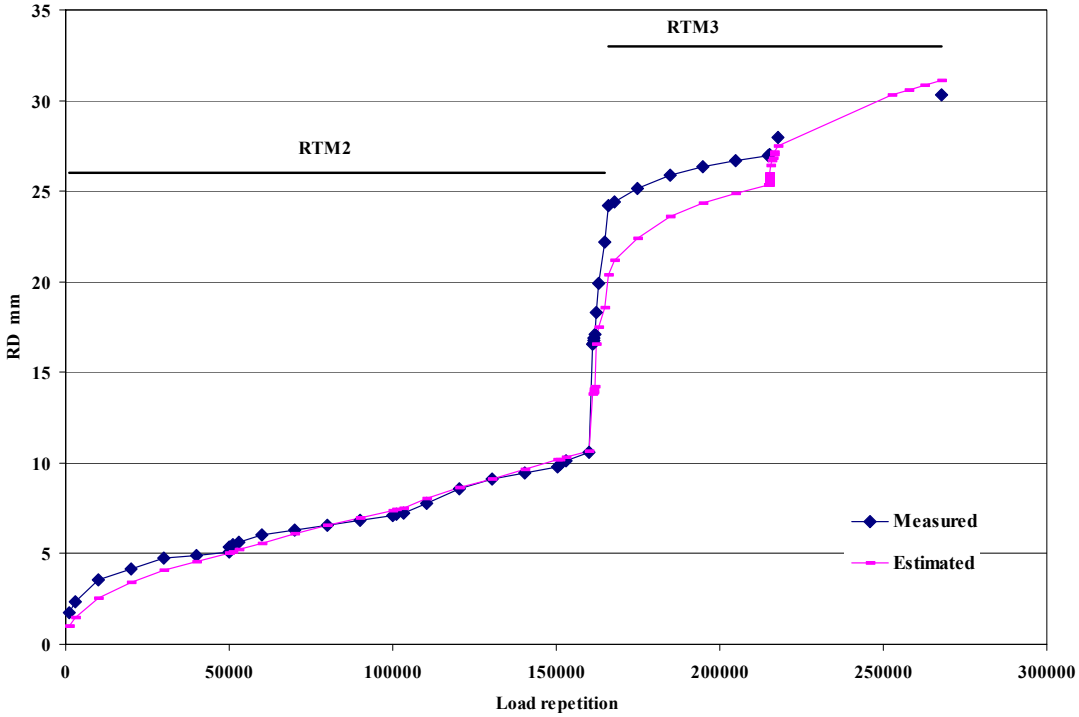

Figure 9. Rut depth (4 foot straight edge) at surface of pavement.

The rut depth is predicted quite well (see Figure 9), even during the first two freeze/thaw experiments.

For the increase in IRI (calculated from the change in surface profile, see Figure 10) the model parameters were:

$$\Delta IRI = 0.64\,m/km \times MN^{0.333} \times \left(\frac{micro\varepsilon}{1000\,micron/m} \right)^{1.333} \times \left(\frac{E}{40MPa} \right)^{0.333}$$

Equation 10

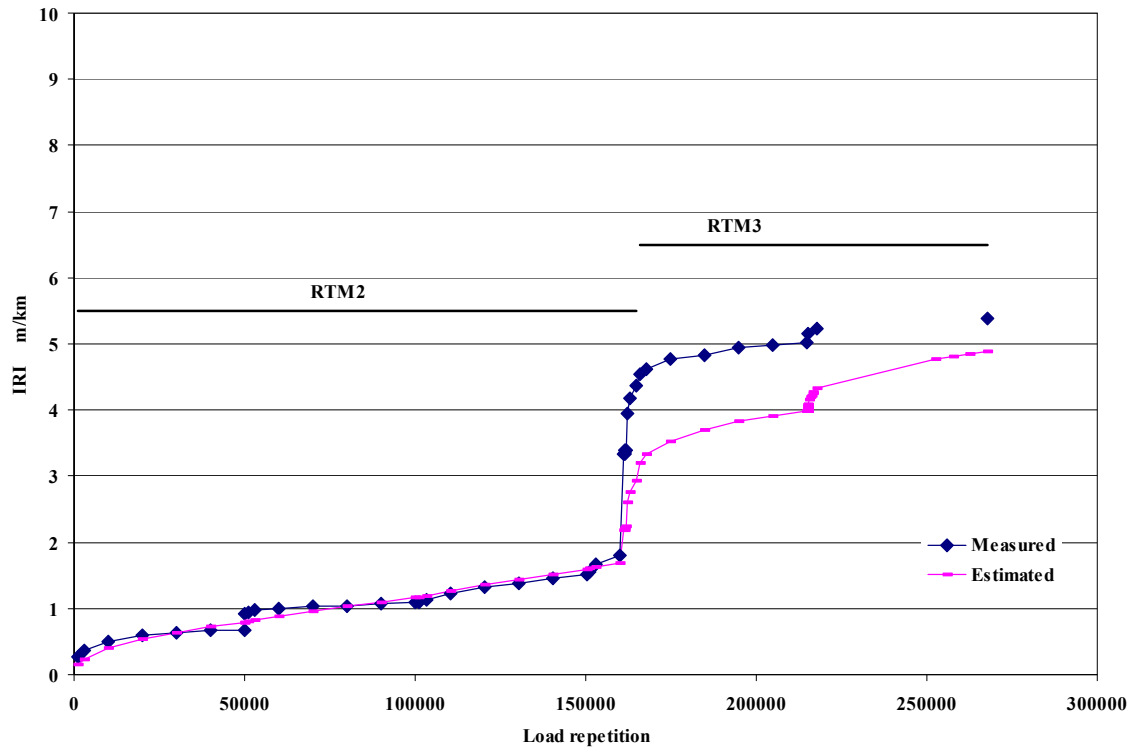

Figure 10. Increase in IRI.

The "classical" Asphalt Institute criterion for subgrade is (Shook et al., 1982):

$$micro\varepsilon_{permissible} = 482\, micron/m \times MN^{-1/4.48}$$

Equation 11

For one million load applications the permissible strain would be 482 microstrain, which should correspond to a rut depth of 12.5 mm (½ inch). For a subgrade material with modulus 40 MPa, one million load applications at this strain level would, however, only result in a rut depth of 1.5 mm, and in 2.1 mm with a modulus of 100 MPa (the same strain at a higher modulus requires a larger stress). Using the climatic conditions with frost given by Shook et al. (2 temperature conditions with 3 soil types each) results in predicted rut depths (from Equation 9) from 1 mm to 2.5 mm. It is evident that the "classical" Asphalt Institute criterion is much more conservative than the simple model.

Conclusion

The damage of an asphalt concrete in terms of the relative decrease in modulus, under direct uniaxial fatigue testing, could be described quite closely using the simple damage model with the parameters given in Equation 2 (or Equation 3), for 16 experiments. The same parameters could be used for controlled strain and controlled stress testing, except for two of the controlled stress tests, where the

agreement was less good. The “classical” Asphalt Institute criterion for asphalt concrete was found to be in reasonably good agreement with the experiments and with the simple model.

The relative decrease in the modulus of a Pozzolan stabilized sand could be described quite well using Equation 5. The decrease in modulus was the result of full scale accelerated loading. The modulus of the stabilized sand was determined from backcalculation of FWD tests. Strains measured at the bottom of the stabilized sand compared well with strains calculated using the layer moduli predicted by the model. When the modulus of the stabilized layer had decreased by about 75% there was no evidence of deterioration at the pavement surface. After the occurrence of the first crack the pavement failed rapidly. The simple model appears to be in reasonably good agreement with French experience with similar materials.

The permanent strain at three levels of two subgrade soils could be described reasonably well by Equation 7, except for the first two freeze/thaw cycles, where the permanent strain was grossly underestimated. Models were also developed for rut depth and IRI. It should be noted that these models are based on the subgrade only, just like “classical” design criteria related to rutting or roughness. It would, of course, be preferable to consider the contribution from each of the pavement layers individually. The simple model was found to be much less conservative than the Asphalt Institute’s criterion for subgrade materials.

References

“French Design Manual for Pavement Structures”, Guide Technique, LCPC 1997.

Monismith, C.L., Ogawa, N., & Freeme, C.R. “Permanent Deformation Characteristics of Subgrade Soils due to Repeated Loading”, Transportation Research Record 537, 1975.

Nilsson, Richard. “Fatigue of Asphalt Mixes – Theory of Viscoelasticity and Continuum Damage Mechanics Applied to Uniaxial Fatigue Data from Laboratory Tests”, Bulletin Highway Engineering 15, Doctoral Thesis, Lund University, 2003.

Shook, J.F., Finn, F.N., Witczak, M.W., & Monismith, C.L. “Thickness Design of Asphalt Pavements – The Asphalt Institute Method”, Proceedings, 5th International Conference on the Structural Design of Asphalt Pavements, Delft 1982.

Ullidtz, P., & Stubstad, R.N. "Analytical-empirical Pavement Evaluation using the Falling Weight Deflectometer", Transportation Research Record 1022, 1985.

Ullidtz, P. “Modelling Flexible Pavement Response and Performance”, Polyteknisk Forlag, 1998.

Zhang, W. & Ullidtz, P. “Estimation of the plastic strain in the pavement subgrade and the pavement functional condition”, Proceedings, 9th International Conference on Asphalt Pavements, Vol 1, Copenhagen 2002.